Essential Role of T-Cell Factor/β-Catenin in Regulation of Rad6B: A Potential Mechanism for Rad6B Overexpression in Breast Cancer Cells

Malathy P.V. Shekhar,[1,2] Larry Tait,[1,2] and Brigitte Gerard[1]

[1]Breast Cancer Program, Karmanos Cancer Institute and [2]Department of Pathology, Wayne State University School of Medicine, Detroit, Michigan

Abstract

We have previously shown that the postreplication DNA repair gene *Rad6B* plays a critical role in the maintenance of genomic integrity of human breast cells. Whereas normal breast cells express low levels of Rad6B, increases in Rad6B expression occur in hyperplasia with overexpression in breast carcinomas. Here, we show that the human *Rad6B* gene is a transcriptional target of T-cell factor (TCF)-4/β-catenin/p300. Rad6B promoter activity is subject to negative regulation in normal human MCF10A breast cells whereas it is constitutively active in metastatic MDA-MB-231 breast cancer cells. Derepression and activation of Rad6B promoter in MCF10A cells require coexpression of β-catenin and p300. Using electrophoresis mobility shift assay, Western blot analysis of electrophoresis mobility shift assay, UV cross-linking, and chromatin immunoprecipitation assay, we show that Rad6B transcriptional repression in MCF10A cells is due to paucity of transcriptionally active β-catenin assembled on the TCF binding sequence in the Rad6B promoter rather than to a deficit/decreased affinity of TCF-4 for the TCF binding element in Rad6B promoter. Three-dimensional epithelial acini generated *in vitro* from MCF10A cells cotransfected with β-catenin and p300 showed β-catenin expression on the membrane, cytoplasm, and/or nuclei with concomitant Rad6 overexpression, whereas control acini showed β-catenin on the membranes and negligible Rad6 expression. Immunohistochemical analysis of 12 breast carcinomas showed an ~80% correlation between Rad6 and β-catenin expression, and combined nuclear and cytoplasmic staining of β-catenin and Rad6 was detected in 25% of the breast carcinomas. *In vivo* implantation of MCF10A-Rad6B cells produced hyperplastic lesions. These data reveal a potentially important role for transcriptionally active β-catenin in the regulation of *Rad6B* gene expression, and link aberrant β-catenin signaling with transcriptional deregulation of Rad6B and breast cancer development. (Mol Cancer Res 2006;4(10):729–45)

Introduction

The Rad6 group is involved in postreplication or "error-prone" repair of DNA (1). The *Rad6* gene encodes a 17-kDa protein (2) and belongs to a group of ubiquitin conjugating enzymes (3) that covalently add ubiquitin to selected lysine residues and commit them to rapid proteolysis. The *Rad6* gene of *Saccharomyces cerevisiae* is required for a variety of cellular functions including DNA repair, induced mutagenesis, and sporulation (4, 5). Rad6-mutant phenotypic effects include slow growth, severe defects in induced mutagenesis, and hypersensitivity to UV, X-ray, chemical mutagens, and antifolate drug metabolites (6). All of the functions by Rad6 protein seem to result from ubiquitination because replacement of the conserved Cys^{88} with Ser produces a totally null phenotype (7, 8).

Rad6 is highly conserved among eukaryotes. Two closely related human homologues of yeast Rad6, HHR6A and HHR6B (referred as Rad6A and Rad6B), encode ubiquitin conjugating enzymes and complement the DNA repair and UV mutagenesis defects of the *S. cerevisiae rad6* mutant (9, 10), but not the sporulation defect, which seems to be dependent on the acidic tail that is found only in the yeast Rad6 (10, 11). Rad6A and Rad6B share 95% identical amino acid identity and are localized on human chromosomes Xq24-q25 and 5q23-q31, respectively (12). Inactivation of the gene encoding Rad6B in mice leads to male sterility (13), whereas male mice lacking Rad6A are fertile (14). Rad6A null female mice fail to produce offspring despite normal ovarian histology and ovulation. The requirement for at least one functional Rad6A or Rad6B allele in all somatic cell types is supported by the fact that male and female mice lacking both homologues and female mice with only one intact Rad6A allele are nonviable (14). Rad6 is associated with centrosomes throughout the cell cycle, implicating its potential role in maintaining fidelity at various phases of cell cycle (15, 16). In this regard, it is interesting to note that constitutive overexpression of Rad6B in normal human breast cells induces centrosome amplification with consequent increase in abnormal mitotic spindle formation, generation of multinucleated cells, aneuploidy, and acquisition of ability for anchorage-independent growth (16). We have previously shown that Rad6B expression level is low in normal human breast tissues; however, detectable increases in Rad6B expression are

Received 5/15/06; revised 8/8/06; accepted 8/10/06.
Grant support: U.S. Army Medical Research and Materiel Command grants DAMD17-99-1-9443 and DAMD-17-02-1-0618 (M.P.V. Shekhar).
The costs of publication of this article were defrayed in part by the payment of page charges. This article must therefore be hereby marked advertisement in accordance with 18 U.S.C. Section 1734 solely to indicate this fact.
Requests for reprints: Malathy P.V. Shekhar, Breast Cancer Program, Karmanos Cancer Institute, 110 East Warren Avenue, Detroit, MI 48201. Phone: 313-833-0715, ext. 2326; Fax: 313-831-7518. E-mail: shekharm@karmanos.org

doi:10.1158/1541-7786.MCR-06-0136

observed in hyperplastic breast lesions and considerable overexpression is observed in breast carcinomas (16). These data suggest that induction of Rad6B expression occurs early during breast carcinogenesis. However, there is little information on mechanisms regulating *Rad6B* gene expression in normal and cancerous breast cells.

The canonical Wnt signaling transduction pathway is involved in many developmental processes as well as in tumor development (17-21). These effects are achieved via activation of the canonical Wnt signaling pathway of downstream target genes by the T-cell factor (TCF)/lymphoid enhancer factor (LEF) family of transcription factors and their coactivator, β-catenin (22). In the absence of Wnt signaling, a multiprotein complex, composed of axin, glycogen synthase kinase 3β, and tumor suppressor adenomatous polyposis coli, phosphorylates β-catenin, leading to its ubiquitin-proteasome–mediated degradation. Wnt signaling negatively regulates the function of this complex and stabilizes β-catenin, which is thereby able to translocate to the nucleus, form a complex with TCF, and induce expression of a variety of TCF target genes (23, 24). TCF/β-catenin–mediated signaling regulates a diverse array of genes that are responsible for cell proliferation, differentiation, migration, and polarity (25). A number of TCF target genes have been identified to date, and these include genes important for development or tumorigenesis. A list of known Wnt/β-catenin–regulated target genes is available online.[3] All these genes contain one or more TCF binding elements in their promoter region near the transcription start site. TCF binding sequences are composed of a highly conserved consensus sequence, 5′-CTTTG[A/T][A/T]-3′, which is recognized by the TCF and LEF family of transcription factors (26, 27). Mutations in β-catenin or other Wnt pathway components, which result in β-catenin accumulation, are found in a wide range of human cancers. In contrast, such mutations have been found only rarely in breast cancer. However, there is strong evidence of stabilization of β-catenin protein in a majority of human breast tumors, implying the existence of an active canonical Wnt signaling pathway in breast carcinomas (28), and studies in mouse model systems show that activated Wnt signaling leads to mammary tumorigenesis (29, 30).

In this study, we show that *Rad6B* gene expression is subject to negative regulation in normal human MCF10A breast cells whereas it is constitutively active in metastatic MDA-MB-231 breast cancer cells. Derepression and activation of the Rad6B promoter in MCF10A cells require coexpression of β-catenin and the coactivator p300. Using electrophoresis mobility shift assay (EMSA), UV cross-linking, and chromatin immunoprecipitation assay, we show that Rad6B transcriptional repression in normal breast cells is due to a paucity of β-catenin/p300 activation complexes assembled on the TCF binding sequence in the Rad6B promoter rather than to a deficit or decreased affinity of TCF-4 for the TCF binding element in the Rad6B promoter. Coexpression of β-catenin and p300 elicits an inductory effect on Rad6B expression in normal MCF10A breast cells. MCF10A cells engineered to constitutively overexpress Rad6B form persistent hyperplastic lesions when xenografted *in vivo* in immunodeficient mice. Immunohistochemical analysis of a small number of breast carcinomas showed a direct correlation between Rad6 and β-catenin expression. Our findings link aberrant β-catenin signaling, a mitogenic pathway, with transcriptional deregulation of Rad6B and implicate Rad6B as an early contributor to breast carcinogenesis.

Results

Overexpression of β-Catenin and p300 Is Required for Derepression of Rad6B Gene Expression

Promoter prediction analysis identified a putative promoter spanning bases −592 to −10 relative to the first ATG codon in the human *Rad6B* gene (Fig. 1). To characterize sequences in the *Rad6B* gene that possess promoter activity, a series of 5′ deletions were made and subcloned into promoterless pGL3 reporter vector (Fig. 1A and B). Reporter constructs were transiently transfected into normal MCF10A and metastatic MDA-MB-231 breast cells. The full-length 5′-Rad6B fragment containing the putative promoter (−722/+9) conferred minimal ability (~4.0-fold higher levels as compared with empty pGL3 vector) to transactivate luciferase reporter gene in MCF10A cells (Fig. 1C). In contrast, similar transfection into MDA-MB-231 cells resulted in ~80-fold higher levels of luciferase gene expression as compared with empty vector (Fig. 1C). 5′ deletion resulted in progressive increases in promoter activity in MCF10A cells; removal of sequences 5′ of −325 (−325/+9 construct; Fig. 1C) resulted in a dramatic induction of luciferase gene expression, which was ~60-fold higher as compared with the intact *Rad6B* gene fragment (Fig. 1C). Similar deletion of sequences 5′ of −325 resulted in ~2.5-fold increase in luciferase gene expression relative to the full-length *Rad6B* gene fragment in MDA-MB-231 cells (Fig. 1C). Further removal of sequences resulted in a complete loss of promoter activity in both MCF10A and MDA-MB-31 cells (Fig. 1C). Such mapping identified a region between nucleotides −325 and −208 that conferred maximal transcriptional induction of luciferase gene expression and, more importantly, the presence of negative regulatory elements located between nucleotides −712 and −325. Because deletion of sequences 5′ of −325 resulted in a dramatic induction (~60-fold) of promoter activity in MCF10A cells, and a modest increase (<3-fold) in MDA-MB-231 cells, our results suggest that *Rad6B* gene expression is regulated by similar *cis* elements in both cell lines but it is under significant negative regulation in normal MCF10A cells as compared with metastatic MDA-MB-231 cells. This difference in Rad6B promoter activity is consistent with decreased levels of Rad6B expression in normal breast cells and its up-regulation in breast cancer cells and tissues (16).

Homologues to known gene regulatory elements in the putative Rad6B promoter were identified using the Mat Inspector program.[4] Many putative *cis* elements were found for ubiquitously expressed transcription factors, including multiple Sp1 and a TCF binding site at nucleotide −341 (Fig. 1A). Deletion of sequences 5′ of −325 involved removal of the TCF binding site with a resultant increase of promoter activity, implying a

[3] http://www.stanford.edu/-musse/pathways/targets.html.

[4] http://www.gene-regulation.com/.

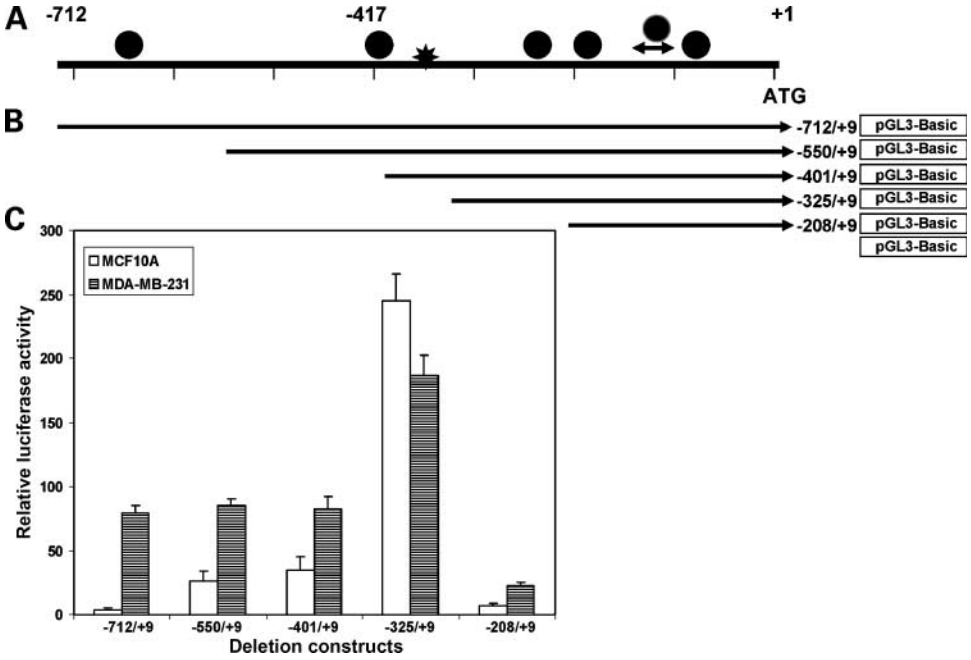

FIGURE 1. Rad6B promoter is subject to negative regulation. **A.** Schematic representation of 5′ untranslated region of *Rad6B* gene. The positions of Sp1 (●) and TCF at −341 (*) relative to the ATG translation start site (+1) are indicated. **B.** Schematic representation of full-length Rad6B promoter (−712) and its various deletion fragments (Rad6B −550, −401, −325, and −208) subcloned into the promoterless pGL3-Basic vector. **C.** The activity of the full-length and various deletion fragments of Rad6B promoter was quantified in transactivation assays in MCF10A or MDA-MB-231 cells. Relative activity levels were normalized to Renilla luciferase activity and corrected for the empty pGL3-Basic vector. Columns, mean of at least six independent experiments; bars, SD.

potential role for TCF in *Rad6B* gene regulation. To gain further insight into the role of TCF in negative regulation of *Rad6B* gene in MCF10A cells, we cotransfected the intact wild-type *Rad6B* gene fragment (−712/+9) with β-catenin (a positive regulator of TCF binding element), p300, or a combination of p300 and β-catenin. Whereas cotransfection with β-catenin or p300 caused a 4- to 7-fold or 4-fold increase in reporter activity, respectively, as compared with the full-length −712/+9 *Rad6B* gene fragment plus empty vectors, cotransfection with a combination of β-catenin and p300 resulted in a synergistic (18-fold) increase in reporter gene expression as compared with full-length *Rad6B* gene fragment plus corresponding empty vectors (Fig. 2A). We further verified the involvement of the TCF binding site at −341 on *Rad6B* gene regulation by site-directed mutagenesis. Transient transfection of MCF10A cells with the full-length *Rad6B* gene fragment containing mutated TCF site at −341 resulted in ∼20-fold induction of basal reporter gene expression as compared with the corresponding wild-type *Rad6B* gene fragment (Fig. 2A). Cotransfection of the mutant promoter construct with p300 induced ∼2- to 3-fold increase in reporter gene expression as compared with the intact mutant *Rad6B* gene fragment. However, similar cotransfections with β-catenin alone or a combination of p300 and β-catenin, unlike that with the wild-type construct, failed to stimulate Rad6B promoter activity (Fig. 2A), thus confirming the responsiveness of the TCF site at −341 to exogenous β-catenin. To confirm that the observed effects are not due to variant sequences 5′ of the TCF regulatory sequence at −341, mutant TCF −401/+9 Rad6B promoter construct that contained the TCF site at −341 but had the 5′ sequences deleted was generated and transfected into MCF10A cells. As observed with the full-length TCF mutant −712/+9 vector, a ∼3.5-fold increase in basal activity was observed with TCF mutant −401/+9 vector as compared with the corresponding wild-type construct, and mutation of −341 TCF site abolished the β-catenin/p300–induced transactivation of Rad6B construct (Fig. 2B). These results indicate that the TCF at −341 plays a dominant role in negative regulation of Rad6B promoter activity. Our data clearly show that transactivation of Rad6B promoter is dependent on activation function of β-catenin and its coactivator p300; however, it is not clear at present why the addition of p300 alone enhanced Rad6B promoter activity.

The functional relevance of TCF in regulation of *Rad6B* gene expression was further confirmed by transient overexpression of ΔN-TCF-4 in MCF10A cells, which resulted in ∼50% inhibition of β-catenin/p300–induced transcriptional activation of reporter from full-length Rad6B promoter, whereas cotransfection of comparable amount of the wild-type TCF-4 had no significant influence (Fig. 2C). Transfection of wild-type TCF-4 at high plasmid concentrations inhibited β-catenin-induced luciferase gene transcription (data not shown), consistent with its transcriptional repressor role when expressed in excess over β-catenin (31, 32). Western blot analysis of β-catenin showed presence of appreciable levels of β-catenin in total cell lysates of MCF10A cells, albeit ∼4- to 5-fold lower than MDA-MB-231 and SW480 cells, respectively (Fig. 2D). Because ectopic expression of ΔN-TCF-4 caused only a 50% decrease of reporter activity, these data suggest that Rad6B promoter repression in MCF10A cells is not due to deficiency of TCF-4 but rather due to limiting amounts of transcriptionally active β-catenin. To confirm this, control experiments were done with pTOP/Flash reporter construct that contains three copies of the consensus wild-type TCF binding sites. Consistent with the results from Rad6B promoter assays (Figs. 1 and 2), transient transfection of MCF10A cells with pTOP/Flash reporter construct yielded very low basal activity; however, expression of exogenous β-catenin resulted in ∼5- to 6-fold increase over control (Fig. 2E and F). Cotransfection with ΔN-TCF-4 inhibited the β-catenin-induced luciferase expression whereas cotransfection of wild-type TCF-4 supported β-catenin-mediated reporter gene expression (Fig. 2F).

Transfection of SW480 colon carcinoma cell line, which expresses high levels of endogenous β-catenin, with pTOP/Flash vector resulted in ~5-fold higher levels of luciferase expression as compared with MCF10A cells (Fig. 2E). Transfections with pFOP/Flash vector that contains mutant TCF binding sites yielded very minimal activity, confirming the functionality and response of TCF binding sites to β-catenin (Fig. 2E).

Analysis of functionality of the Rad6B TCF binding site in metastatic MDA-MB-231 cells showed that the full-length −712/+9 Rad6B promoter is induced ~2.0-fold by ectopic expression of β-catenin and p300 (Fig. 2G) as compared with ~18-fold in MCF10A cells (Fig. 2A). Inclusion of ΔN-TCF-4 caused ~66% inhibition of basal activity of the full-length Rad6B promoter, and this inhibition was sustained in the presence of exogenous β-catenin/p300. Coexpression of wild-type TCF-4 did not significantly influence β-catenin/p300–induced reporter gene expression (Fig. 2G). Transfection of the TCF mutant −712/+9 Rad6B promoter in MDA-MB-231 cells resulted in >2-fold increase in basal activity of the intact Rad6B promoter fragment, which is uninfluenced by ectopic expression of ΔN-TCF-4, β-catenin/p300, or wild-type TCF-4 (Fig. 2G). These data suggest that the Rad6B promoter activity in MDA-MB-231 cells is also subject to similar regulation by TCF/β-catenin/p300 as in MCF10A cells; however, unlike in MCF10A cells, the Rad6B promoter is largely derepressed in MDA-MB-231 cells as observed by very small increases in basal reporter activity by exogenous β-catenin/p300 and greater inhibition by ΔN-TCF-4 (Fig. 2F).

Activation of the Rad6B Promoter by β-Catenin/p300 Results in Elevated Levels of Rad6B

Because results of promoter assays implicated an important functional role for TCF/β-catenin/p300 on *Rad6B* gene expression, we assessed the effects of ectopic β-catenin and p300 expression on *Rad6B* gene expression in MCF10A cells. Rad6B mRNA levels detected by semiquantitative reverse transcription-PCR (RT-PCR) analysis showed ~2.8-fold higher levels of Rad6B mRNA levels in β-catenin/p300–transfected MCF10A cells as compared with corresponding vector control. Inclusion of ΔN-TCF4 inhibited β-catenin/p300–induced increase in Rad6B mRNA (Fig. 3A). Higher levels of Rad6B mRNA induction are possibly not detected because *Rad6B* transcripts have a short half-life, consequently failing to accumulate appreciable steady-state levels; however, the translated Rad6B protein is stable (15). Western blot analysis of Rad6B protein levels showed ~3- to 5-fold increase in MCF10A cells transfected with a combination of β-catenin and p300 as compared with corresponding vector control. Contrary to the results from promoter assays (Fig. 2), transfections with either the p300 or β-catenin expression vector did not significantly induce Rad6B protein expression (Fig. 3B).

To further evaluate the effects of ectopic β-catenin and p300 on Rad6 protein expression and localization in epithelial acini, single-cell suspensions of MCF10A cells were transiently transfected in suspension with β-catenin/p300 or control vectors, and three-dimensional acini were generated by plating the transfected cells in reconstituted basement membrane matrix (Matrigel). After 5 to 7 days in culture, each cell formed an acinus consisting of 8 to 20 cells (Fig. 3C). Immunostaining of control acini showed weak immunoreactivity to Rad6 (Fig. 3C, *c*) and β-catenin reactivity was confined to the cell membranes (Fig. 3C, *b*). In acini generated from β-catenin/p300–transfected MCF10A cells, the cell-cell junction marker β-catenin was found in the cytoplasm and/or nuclei besides being localized on the cell membranes (Fig. 3C, *e*). Consistent with our data from promoter assays and Western blot analysis, β-catenin/p300 transfection induced Rad6 expression as revealed by intense immunoreactivity to Rad6 antibody in β-catenin/p300–transfected MCF10A acini (Fig. 3C, compare *c* and *f*). Also consistent with the data from MCF10A acini, immunofluorescence staining of β-catenin in monolayers established in parallel with the three-dimensional experiment showed intense staining of β-catenin on the cell membranes

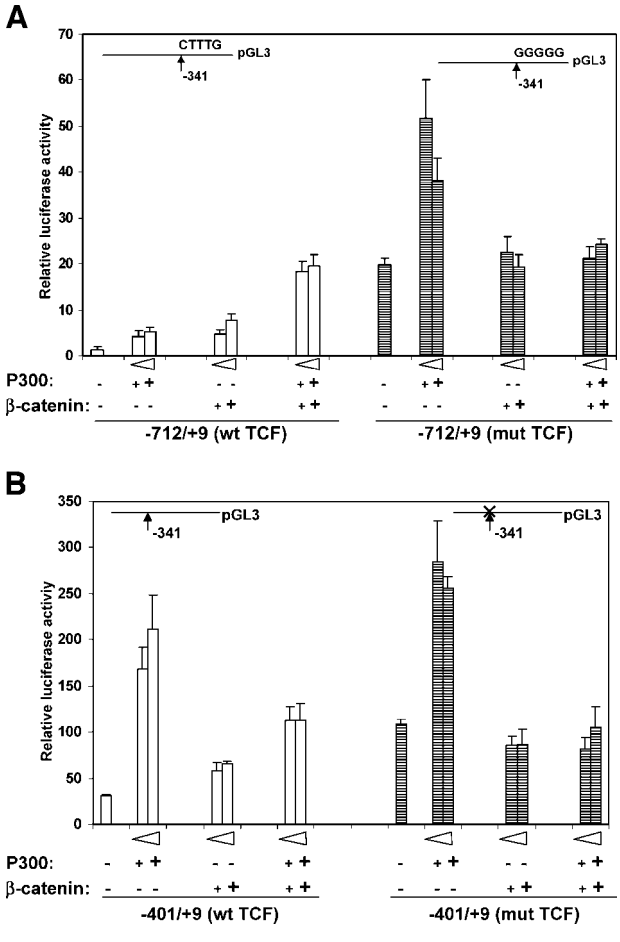

FIGURE 2. Identification of the TCF binding sequence in the Rad6B promoter. The activity of the full-length Rad6B promoter −712 carrying wild-type TCF binding site (CTTTGAA) and site-directed mutation of the TCF site (GGGGGAA) at −341 (**A**) or the Rad6B deletion construct −401 containing wild-type or the mutated (GGGGGAA) TCF site at −341 (**B**) was quantified in transactivation assays in MCF10A cells. β-Catenin or p300, 0.25 (1×) or 0.5 μg (2×) each, or a combination of p300 and β-catenin, or their corresponding control plasmids were cotransfected with either full-length (−712/+9 wild-type or mutant TCF) or deletion (−401/+9 wild-type or mutant TCF) Rad6B promoter constructs. DNA concentrations were kept constant with empty vector DNA. Columns, mean of at least six independent experiments; bars, SD.

(with associated membrane ruffling) and perinuclear staining and/or nuclear staining of β-catenin/p300–transfected MCF10A cells. In contrast, in empty vector–transfected MCF10A cells, β-catenin was predominantly localized on the cell membranes (without discernible membrane ruffling) and was absent or only very weakly detectable in the cytoplasm (Fig. 3C, *a* and *d*). It is interesting to note that ectopically expressed β-catenin persists in MCF10A acini at 6 days posttransfection, suggesting that the

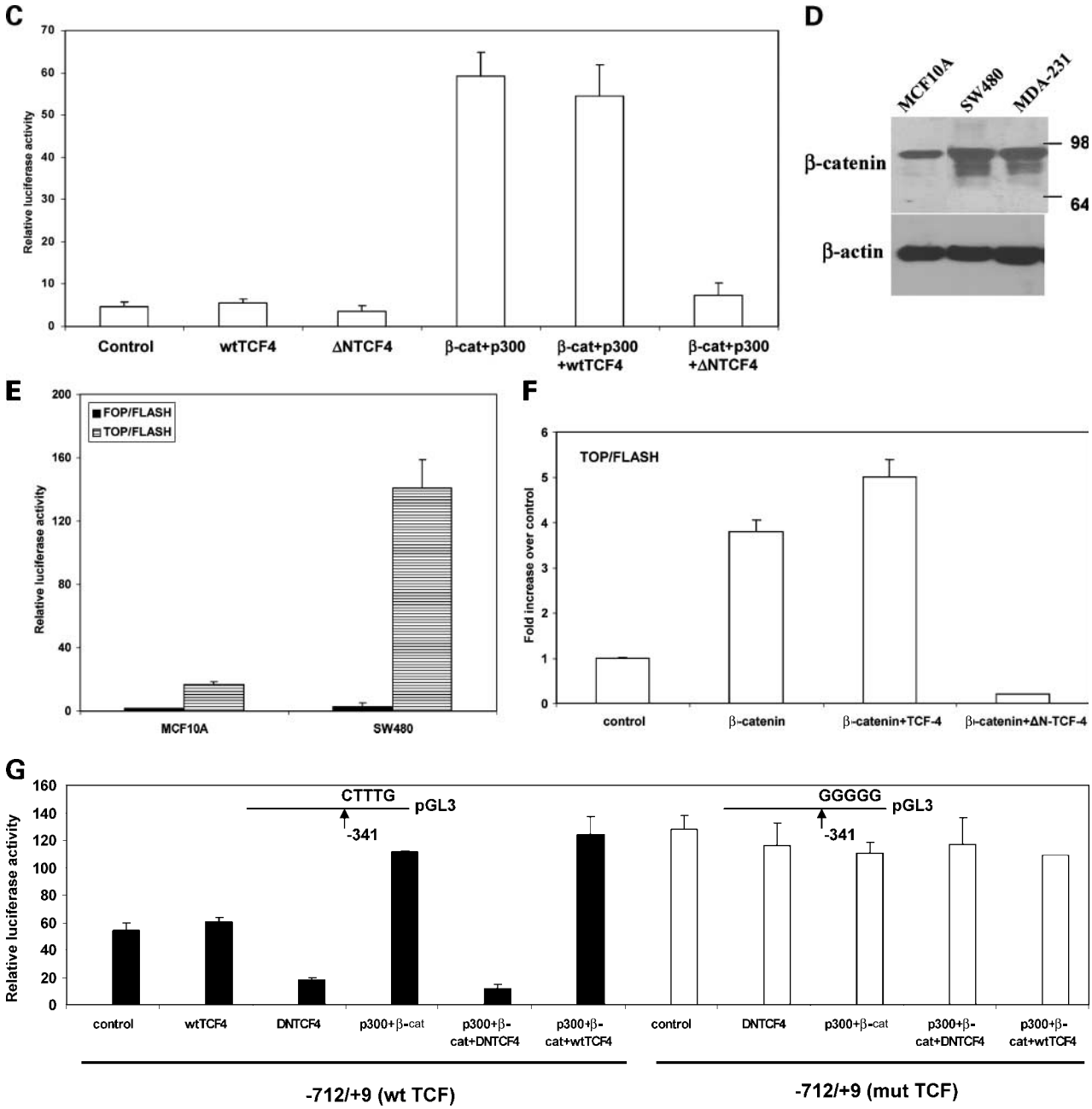

FIGURE 2 *Continued.* **C.** The activity of the full-length Rad6B promoter (−712) construct in the presence of expression vectors for wild-type TCF-4, ΔN-TCF-4, p300 + β-catenin, or p300 + β-catenin with wild-type TCF-4 or ΔN-TCF-4, or the corresponding control plasmids was measured in MCF10A cells. Columns, mean of four independent experiments; bars, SD. **D.** Steady-state levels of β-catenin in MCF10A, MDA-MB-231, and SW480 total cell lysates relative to β-actin. **E.** The transcriptional activity of endogenous β-catenin in MCF10A cells was assessed by transfection of TOP/FLASH or FOP/FLASH reporter vector. Similar transfections were done in SW480 colon carcinoma cells that served as positive control. Activity was normalized against Renilla luciferase activity. Columns, mean of four independent experiments; bars, SD. **F.** The effects of β-catenin, β-catenin + wild-type TCF-4, or β-catenin + ΔN-TCF-4, or the corresponding control plasmids on the activity of TOP/FLASH vector was measured in MCF10A cells. Columns, mean of four independent experiments; bars, SD. **G.** The activity of the full-length Rad6B promoter −712 carrying wild-type TCF binding site (CTTTGAA) and site-directed mutation of the TCF site (GGGGGAA) at −341 was tested in MDA-MB-231 cells in the presence of ΔN-TCF-4, wild-type TCF-4, β-catenin/p300, ΔN-TCF-4 plus β-catenin/p300, or wild-type TCF-4 plus β-catenin/p300 and compared with those transfected with corresponding empty vectors. Activity was normalized against Renilla luciferase activity. Columns, mean of three independent experiments; bars, SD.

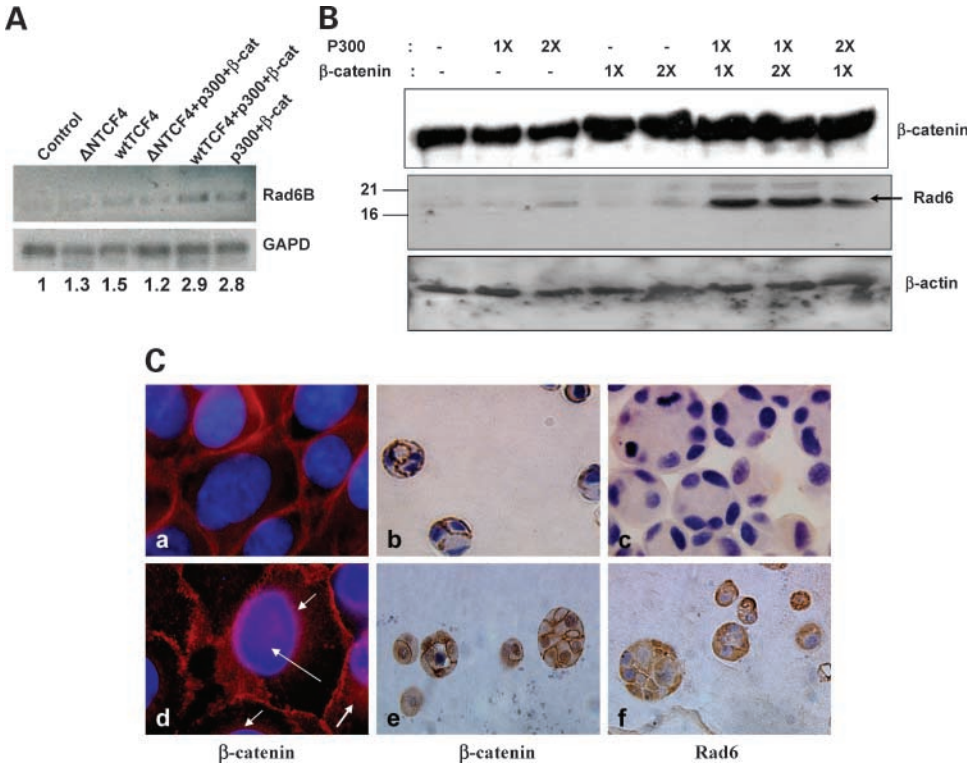

FIGURE 3. Levels of Rad6B mRNA (**A**) and protein (**B**) were measured by semiquantitative RT-PCR or Western blot analysis from total RNA or cell lysates, respectively, prepared from MCF10A cells transfected in parallel with Fig. 2C. **B.** Because the antibody may not distinguish the two forms of very closely related Rad6A and Rad6B proteins, immunoreactive Rad6 proteins detected with this antibody are referred to as Rad6 rather than Rad6A or Rad6B. **C.** MCF10A cells transiently transfected with empty vectors (*a-c*) or β-catenin/p300 (*d-f*) were seeded on coverslips to generate monolayers (*a* and *d*) or suspended in Matrigel to generate epithelial acini (*b, c, e*, and *f*). Acini generated from MCF10A cells transfected with β-catenin/p300 (*e* and *f*) or the corresponding control plasmids (*b* and *c*) were fixed in buffered formalin, paraffin embedded, and sections stained with antibodies to β-catenin (*b* and *e*) or Rad6 (*c* and *f*). p300 expression/distribution is not shown because the p300 antibody was not suitable for immunostaining. Note that immunofluorescence staining of corresponding monolayers revealed intense β-catenin immunoreactivity on the cell membranes, ruffling of cell membranes, and perinuclear (*short arrow*; *d*) or nuclear (*long arrow*; *d*) staining of β-catenin/p300–transfected MCF10A cells (*d*).

expressed β-catenin protein is stable and functionally active, as supported by elevated expression of β-catenin and Rad6. A plausible explanation for this is that MCF10A cells organized into acinar structures display very low (~10-fold lower) proliferation rates as compared with those in monolayers, thus potentially prolonging the stability of transiently expressed proteins.

TCF/β-Catenin Complex Formation with Rad6B TCF Binding Sequence Is Detected in MDA-MB-231 Cells but not in MCF10A Cells

To determine whether the TCF binding element identified by promoter assays can indeed bind to TCF/β-catenin heterodimer, we conducted EMSA using the wild-type TCF binding site of the Rad6B promoter and a corresponding sequence containing mutant TCF binding site. Figure 4 shows that nuclear proteins from MCF10A and MDA-MB-231 cells exhibit different patterns of complex formation when incubated with the TCF binding sequence of Rad6B promoter. Specific complexes B to D formed with MCF10A nuclear proteins (Fig. 4A, *lane 1*) migrate faster as compared with specific complexes 1 to 4 formed by MDA-MB-231 nuclear proteins (Fig. 4A, *lane 4*). The complexes formed are specific for the wild-type TCF binding sequence as the corresponding double-stranded oligonucleotides with mutation in the TCF binding site are unable to compete (Fig. 4A, *lanes 2* and *7*; Fig. 4B, *lanes 3* and *11*), but are readily competed by a 10-fold (Fig. 4A, *lanes 3* and *5*) or 50-fold (Fig. 4A, *lane 6*; Fig. 4B, *lane 2*) molar excess of the unlabeled wild-type probe. In contrast, the slow-migrating complex A formed from MCF10A nuclear proteins is competed less efficiently by the unlabeled wild-type competitor because addition of 50-fold molar excess of the wild-type competitor caused only ~50% decrease in complex A but inhibited complexes B to D by >90% (Fig. 4B, compare *lanes 1* and *2*). Addition of β-catenin antibody to binding reactions selectively inhibited the formation of all four specific complexes formed from MDA-MB-231 nuclear proteins (Fig. 4B, *lane 7*), whereas it had no effect on complexes formed from MCF10A nuclear extracts (Fig. 4B, *lane 4*). Inclusion of TCF-4 antibody inhibited formation of complex 1 in MDA-MB-231 cells (Fig. 4B, *lane 13*) but had no effect on complexes 3 and 4 (Fig. 4B, *lane 13*). Because complex 2 is more diffuse, we are unable to confirm the effect of TCF-4 antibody on complex 2. Incubation with preimmune immunoglobulin G (IgG) did not influence formation or stability of

the complexes (Fig. 4B, *lanes 5, 8, 14*, and *16*). These results suggest that complexes 1 to 4 formed from MDA-MB-231 nuclear proteins contain β-catenin whereas TCF-4 is present mainly in complex 1 and is not part of complexes 3 and 4. Thus, other complexes containing β-catenin probably contain other isoforms of TCF. Addition of TCF-4 antibody to MCF10A binding reactions had no effect on complex A formation, weakly affected complexes C and D, and inhibited complex B formation (Fig. 4, *lane 17*). The results from EMSAs are consistent with our observation that MCF10A cells possess weak Rad6B promoter activity due to deficit of transcriptionally active β-catenin assembled on the Rad6B TCF binding sequence despite the presence of significant amounts of β-catenin in MCF10A whole-cell extracts (Fig. 2D).

Because addition of anti-β-catenin or anti-TCF-4 antibodies caused interference of specific complex formation rather than supershifts, we further verified the presence of TCF-4 and β-catenin in DNA-protein complexes formed in EMSAs by direct Western blotting and UV cross-linking analysis. Direct Western blot analysis of EMSA (Fig. 5A) confirmed the presence of β-catenin and TCF-4 in complexes formed from MDA-MB-231 nuclear proteins and showed that whereas β-catenin is detectable in complexes 1, 3, and 4, the majority of it is associated with the slow-migrating complex 1 (Fig. 5B). Three TCF-4 immunoreactive bands were observed; the most intense band was associated with complex 1 whereas the other two bands seemed to be part of complex 2 (Fig. 5C). β-Catenin and TCF-4 coexist in complex 1 whereas TCF-4 immunoreactivity is not detected in complexes 3 and 4 (Fig. 5B and C). These results suggest that β-catenin-containing complexes 3 and 4 probably contain other TCF isoforms. Neither TCF-4 nor β-catenin immunoreactive complexes were found in EMSA reactions from MCF10A nuclear extracts; it is very likely that faster-migrating TCF-4-containing complexes could have been missed under the conditions employed to locate the slow-migrating bands in mini polyacrylamide gels (Fig. 5B and C).

To further verify and assess the approximate molecular masses of the DNA-protein complexes formed from MCF10A and MDA-MB-231 nuclear extracts, UV cross-linked EMSA products were analyzed on SDS-PAGE. UV cross-linked complexes with molecular masses of ~75 and >250 kDa were observed in MDA-MB-231 binding reactions, whereas only the 75-kDa band was observed in MCF10A binding reactions (Fig. 6A). Incubation of the binding reactions with 50-fold molar excess of unlabeled probe before UV cross-linking abolished formation of both the bands, indicating their specificity (Fig. 6A, *lanes 4* and *3*). Western blot analysis of the UV cross-linked reactions with anti-β-catenin (Fig. 6B) or anti-TCF-4 (Fig. 6C) antibodies showed that the larger >250-kDa complex contained both β-catenin (Fig. 6B, *lane 2′*) and TCF-4 (Fig. 6C, *lane 2′*), whereas the 75-kDa complex contained only TCF-4 (Fig. 6C, *lanes 2* and *2′*). Because equivalent amounts of TCF-4 immunoreactivities were observed in the 75-kDa complex formed from MCF10A and MDA-MB-231 UV cross-linked samples (Fig. 6C, compare *lanes 2* and *2′*), these results suggest that TCF-4 proteins in MCF10A and MDA-MB-231 nuclear extracts exhibit similar binding affinities for the TCF site on the Rad6B promoter. These

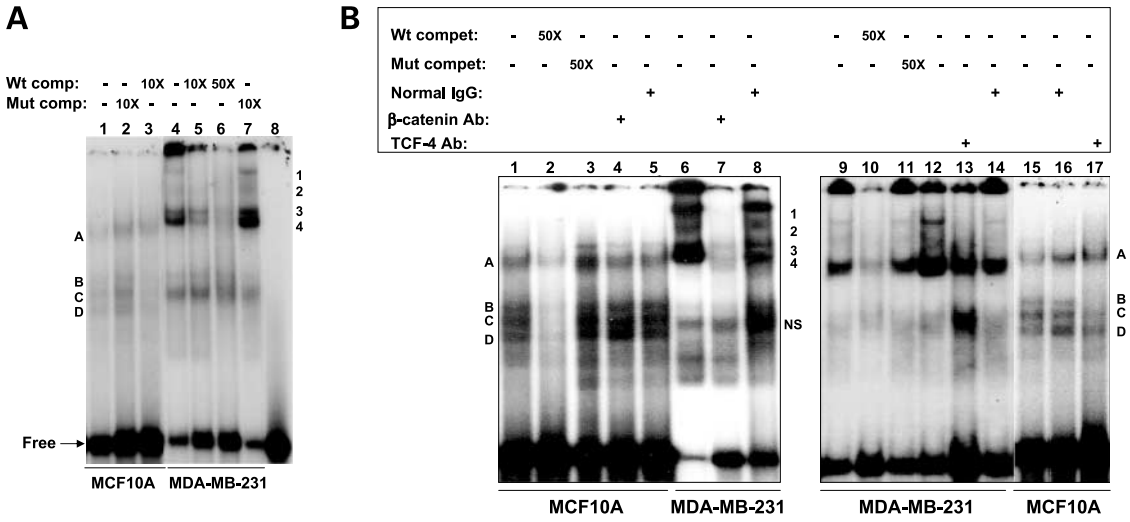

FIGURE 4. *In vitro* binding activity of MCF10A and MDA-MB-231 nuclear proteins to human Rad6B promoter. Duplex oligonucleotides containing the putative (−341) TCF binding sequence of the Rad6B promoter were end labeled and incubated with 10 μg of MCF10A or MDA-MB-231 nuclear proteins. The positions of specific retardations are indicated by complexes A to D for MCF10A cells and complexes 1 to 4 for MDA-MB-231 cells. **A.** Nuclear proteins were incubated with labeled Rad6B probe or with 10-fold (*10×*) or 50-fold (*50×*) molar excess of unlabeled Rad6B sequences [containing wild-type TCF (*Wt*) or mutant TCF (*Mut*)] as competitors. Lane 8 contained only the radiolabeled probe. **B.** MCF10A or MDA-MB-231 nuclear proteins were incubated with 0.5 μg of β-catenin antibody or TCF-4 antibody in the binding reaction mixture before the addition of labeled Rad6B probe. Equivalent amounts of mouse or rabbit preimmune IgG were added as control (*lanes 5, 8, 14*, and *16*). Note that addition of β-catenin antibody severely inhibited formation of specific complexes 1 to 4 without any effect on nonspecific complexes (*NS*; compare *lanes 6* and *7*), whereas inclusion of normal IgG did not affect complexes 1 to 4 (*lane 8*). Similar addition of anti-β-catenin antibody had no effect on complexes formed from MCF10A nuclear proteins (compare *lanes 1, 4*, and *5*). Addition of anti-TCF-4 antibody to MDA-MB-231 reactions inhibited complex 1 without any effect on complex 3 or 4, whereas inclusion of the corresponding normal IgG had no effect (compare *lanes 9* and *12* with *lanes 13* and *14*). Lane 12 contains 20 μg of MDA-MB-231 nuclear proteins. Addition of TCF-4 antibody to MCF10A reactions inhibited complex B, weakly affected complexes C and D, and had no effect on complex A (compare *lanes 15* and *16* with *lane 17*).

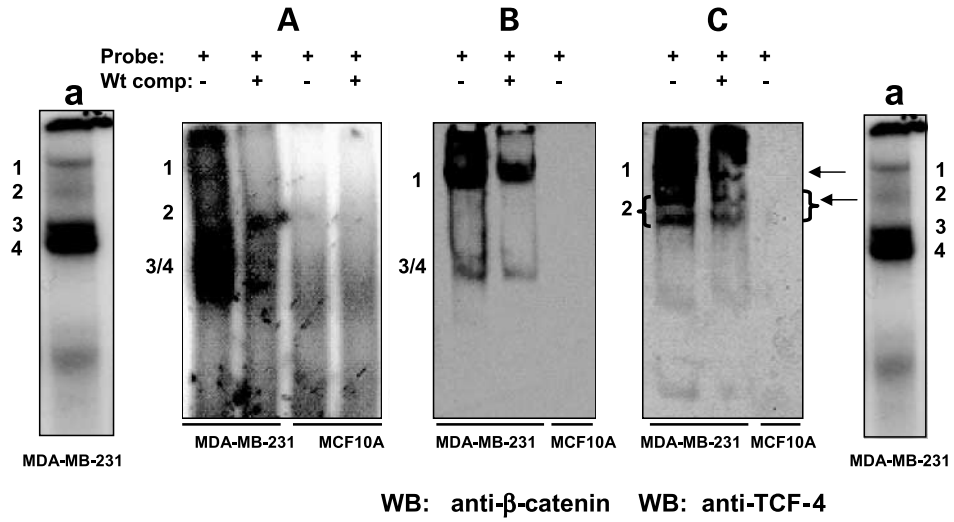

FIGURE 5. Direct Western blot analysis of EMSA of the Rad6B promoter. MCF10A or MDA-MB-231 nuclear extracts were incubated with radiolabeled Rad6B promoter fragment in the presence or absence of a 50-fold molar excess of corresponding unlabeled wild-type competitor. Complexes were separated and either subjected to autoradiography (**A**) or transferred to nitrocellulose for Western blot analysis (**B** and **C**) with anti-β-catenin (**B**) or anti-TCF-4 (**C**) antibody. The positions of specific complexes 1 to 4 formed with MDA-MB-231 nuclear proteins and separated on large gels (*a*) are shown for comparison of mobilities of corresponding complexes separated on mini gels (**A-C**). The specific complexes formed between the Rad6B probe and MCF10A nuclear proteins are not seen on EMSA done in mini gels because the electrophoretic conditions were set for attaining optimal separation of slower migrating complexes 1 to 4, which resulted in loss of the faster-migrating specific complexes formed with MCF10A nuclear proteins (Fig. 4). Because β-catenin and TCF-4 immunoreactivities are seen as a smear (besides the defined complex 1 band) running up to the top of the gel, it is likely that they contain high molecular weight proteins such as p300 or additional proteins.

results also suggest that the observed differences in Rad6B promoter activities between MCF10A and MDA-MB-231 cells arise from differences in functional levels and/or activity of nuclear β-catenin, which is capable of binding to the Rad6B promoter (Fig. 6B, *lanes 1, 2* and *1′, 2′*). It is interesting to note that although similar amounts of MCF10A or MDA-MB-231 nuclear proteins were used in each reaction, TCF-4 immunoreactivity was significantly enhanced in UV cross-linked reactions containing Rad6B DNA probe as compared with non-cross-linked reactions (Fig. 6C, compare *lanes 1* and *2* and *lanes 1′* and *2′*). These results suggest that the TCF-4 epitope at its COOH terminus is probably rendered more accessible to the antibody when TCF-4 is complexed with Rad6B DNA.

To confirm whether *in vivo* differences in complex formation at the TCF-site do indeed account for Rad6B promoter repression or constitutive activity in MCF10A and MDA-MB-231 cells, respectively, we did chromatin immunoprecipitation assays on MCF10A and MDA-MB-231 cells. Using chromatin immunoprecipitation with anti-TCF-4

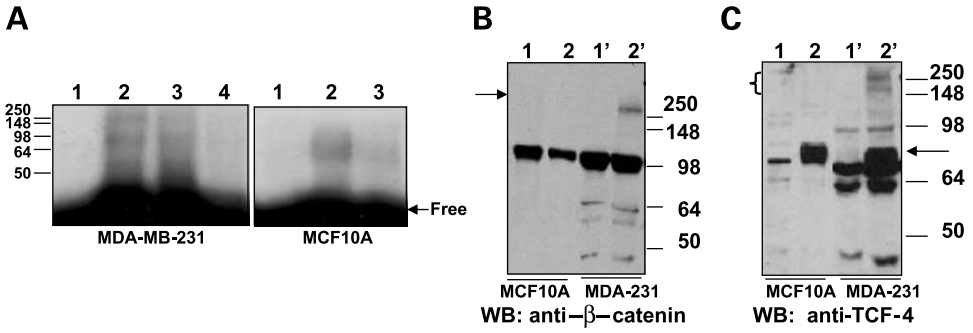

FIGURE 6. Analysis of UV cross-linked EMSA of the Rad6B promoter. MCF10A or MDA-MB-231 nuclear proteins were incubated with radiolabeled Rad6B promoter probe in the presence or absence of unlabeled wild-type Rad6B competitor. UV-irradiated as well as corresponding nonirradiated binding reactions were separated and subjected to autoradiography (**A**) or Western blot analysis with β-catenin (**B**) or TCF-4 (**C**) antibodies. Lane 1, binding reaction without UV cross-linking; lane 2, binding reaction with UV irradiation; lanes 3 and 4, binding reactions incubated in the presence of a 10- or 50-fold molar excess of unlabeled competitor, respectively. **B** and **C.** Lanes 1, 2 and 1′, 2′, binding reactions with MCF10A and MDA-MB-231 nuclear extracts, respectively. **B.** A specific >250-kDa UV cross-linked β-catenin reactive band (*arrow, lane 2′*) was detected only with MDA-MB-231 extracts, which is not detected in nonirradiated reactions (*lane 1′*). **C.** Western blot analysis with TCF-4 antibody showed the presence of a specific UV cross-linked band of ~75 kDa (*arrow*) with both MCF10A and MDA-MB-231 nuclear extracts (*lanes 2* and *2′*) whereas this band was not detected in nonirradiated reactions (*lanes 1* and *1′*). Note the presence of TCF-4 immunoreactive bands >250 kDa (as in **B**) with MDA-MB-231 nuclear proteins (*lane 2′, bracket*).

antibody followed by Western blot with anti-β-catenin or anti-p300 antibodies, we examined the *in vivo* occupancy of the TCF site (−341) by TCF-4 on the one hand and formation of a TCF-4/β-catenin/p300 complex on the other hand (Fig. 7A and B-*c*). Chromatin immunoprecipitation done with anti-β-catenin antibody showed the absence of β-catenin at the TCF site in control MCF10A cells (Fig. 7B-*b*); however, β-catenin occupancy of the TCF site was triggered in MCF10A cells that were cotransfected with β-catenin and p300 expression vectors (Fig. 7A and B-*c*). In contrast, the TCF site was occupied by β-catenin in MDA-MB-231 cells (Fig. 7A and B-*b*). No PCR product was amplified with β-catenin chromatin immunoprecipitation from Rad6B promoter region circumventing the TCF binding site (Fig. 7B, *a*). Chromatin immunoprecipitation experiments done with anti-β-catenin antibody showed β-catenin occupancy of the TCF binding site on the cyclin D1 promoter in MDA-MB-231 cells but not in MCF10A cells (Fig. 7C). These data confirm that MCF10A cells are deficient in transcriptionally active β-catenin, and that β-catenin recruitment to the TCF binding site in the Rad6B promoter is critical for formation of an "on TCF (−341)" β-catenin/p300 complex and stimulation of Rad6B promoter activity.

Constitutive Overexpression of Rad6B in Normal Breast Cells Induces Formation of Hyperplastic Lesions In vivo

Normal MCF10A cells stably transfected with human Rad6B expression vector produced persistent lesions with benign hyperplasia (grade 2) in 9 of 10 mice and differentiated carcinoma (grade 5) in 1 of 10 mice when injected into the mammary fatpads of immunodeficient female nude mice, whereas the corresponding vector control MCF10A-Neo cells failed to grow *in vivo* (ref. 33; Fig. 8A). Subcutaneous injection of MCF10A-Rad6B cells into an ectopic site, such as the flanks, also produced hyperplastic lesions in five of five mice, similar to those observed at the orthotopic site, and indicates

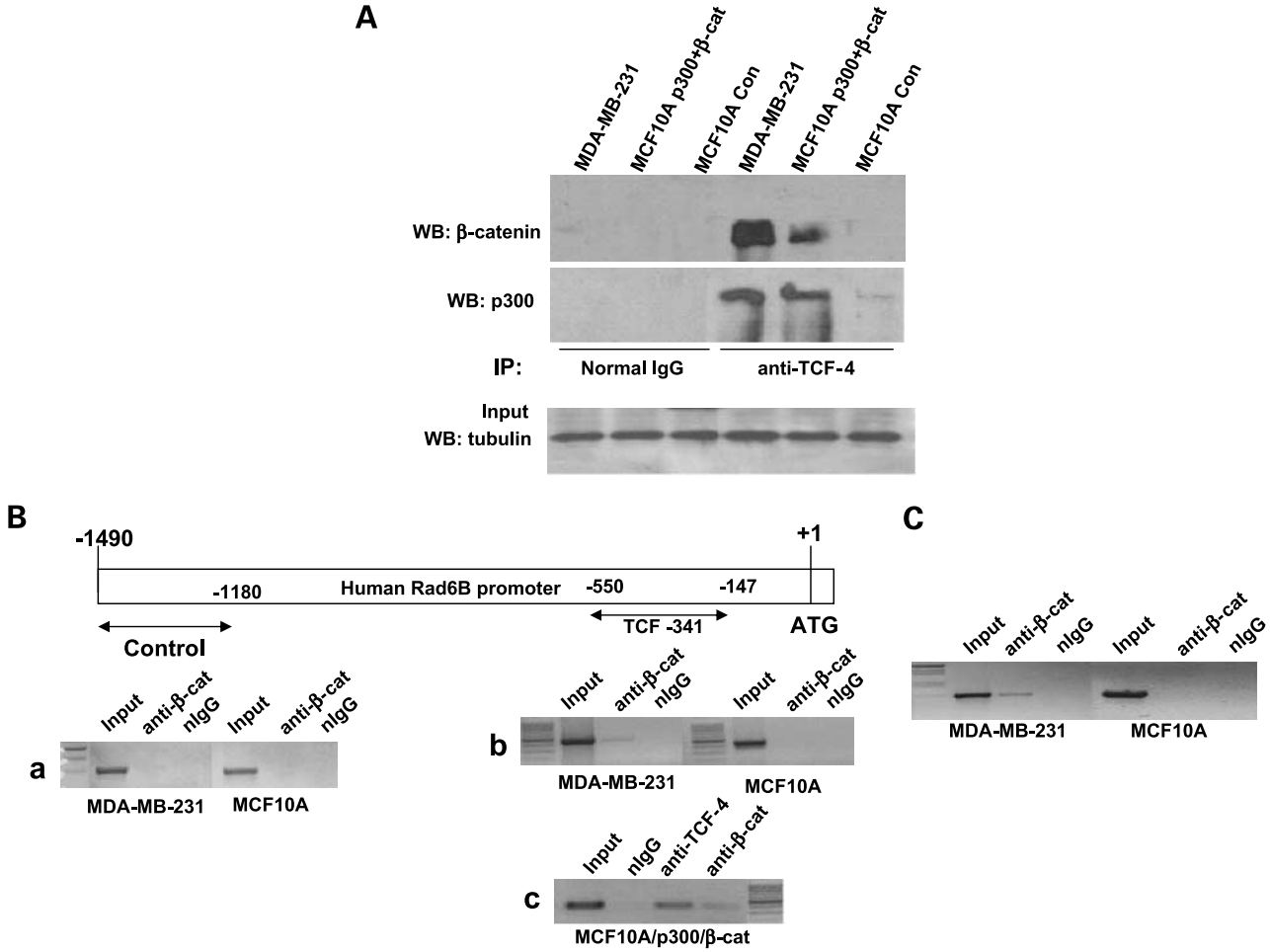

FIGURE 7. Rad6B promoter is occupied by β-catenin in MDA-MB-231 cells but not in MCF10A cells. **A.** Chromatin immunoprecipitation was done on MCF10A, MCF10A cotransfected with p300 and β-catenin expression plasmids, or MDA-MB-231 cells with anti-TCF-4 antibody or the corresponding normal IgG, followed by Western blot analysis with anti-β-catenin or anti-p300 antibodies, or PCR amplification (**B**, *c*). Before chromatin immunoprecipitation, equal input was verified by immunoblotting with anti-tubulin antibody. **B.** Chromatin immunoprecipitation done on MCF10A and MDA-MB-231 cells (*a* and *b*) or MCF10A cells cotransfected with p300 and β-catenin (*c*). **C.** Chromatin immunoprecipitation assays done with anti-β-catenin antibody on MCF10A and MDA-MB-231 cells were PCR amplified with primers (bases 880-1,410; accession no. AF511593) encompassing the TCF [1351] site of the human cyclin D1 gene. The TCF [1351] site on cyclin D1 promoter is occupied by β-catenin in MDA-MB-231 but not in MCF10A cells.

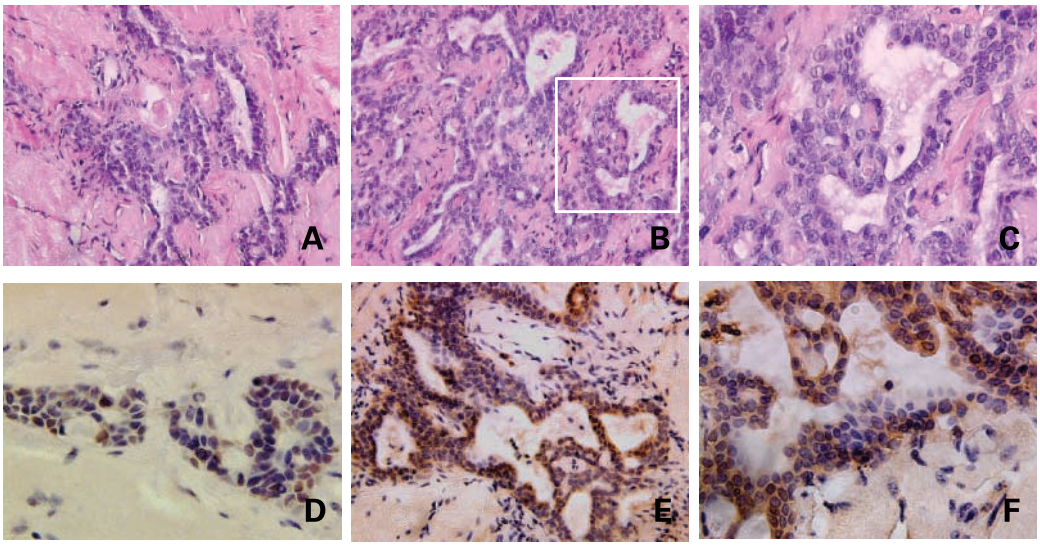

FIGURE 8. Constitutive overexpression of Rad6B in MCF10A cells induces hyperplasia. MCF10A cells stably transfected with Rad6B expression vector or their corresponding empty vector (16) were injected subcutaneously into the mammary fatpads (**A**) or flanks (**B** and **C**) of female nude mice. Lesions were harvested at 10 weeks, fixed, and paraffin embedded. Sections were stained with H&E (**A-C**), anti–proliferating cell nuclear antigen (**D**), or anti-Rad6 antibody (**E** and **F**). **C**. Magnified version of the outlined box in **B**. Vector control MCF10A cells fail to grow *in vivo* and hence are not shown. Magnification, ×20 (**A, B**, and **E**); ×40 (**C, D**, and **F**).

that the hyperplastic ducts are not derived from the mouse mammary glands (Fig. 8B and C). Additionally, cell cultures established from xenografts retained the characteristic translocation markers t(5;9) and t(3;17) and trisomy 20 found in MCF10A-Rad6B cells (16). The ducts generated from MCF10A-Rad6B cells showed disordered epithelial growth, and the epithelium was at least two or more layers thick. Hyperplasia affected the entire epithelium circumferentially in some ducts, whereas in others, it affected a segment of the ducts (Fig. 8A-C). The hyperplastic lesions retained strong Rad6 expression of MCF10A-Rad6B cells as revealed by immunohistochemical analysis of xenografts with anti-Rad6 antibody (Fig. 8E and F). Immunostaining with anti–proliferating cell nuclear antigen antibody revealed the proliferative potential of hyperplastic ducts formed from MCF10A-Rad6B cells as >30% of the nuclei stained positively for proliferating cell nuclear antigen (Fig. 8D). These results are consistent with our previous data that the first detectable increase in Rad6 protein expression develops in benign breast hyperplasias (16), and point to a role for Rad6B in early breast carcinogenesis.

Breast Carcinomas Display a Correlation between Rad6 and β-Catenin Expression

Because our results from reporter-based assays have indicated a transcriptional regulatory role for β-catenin on *Rad6B* gene expression, we analyzed whether the expression of Rad6 in breast tumors is related with β-catenin overexpression. The presence of an association between Rad6 and β-catenin expression was characterized in 12 breast carcinomas. In agreement with our previously reported results (16), low levels of Rad6 protein were detected in normal ducts of normal breast (data not shown) and in nontumorous ducts from breast cancer tissue (Fig. 9A). Also consistent with our previous data (16), breast tissues with adenosis exhibited moderate cytoplasmic Rad6 reactivity (Fig. 9B), and breast tumors with ductal carcinoma *in situ* or invasive cancer displayed intense Rad6 reactivity that was localized in the cytoplasm (Fig. 9E) or combined cytoplasm and nuclei (Fig. 9C and D). We speculate that abundant localization of Rad6, a postreplication DNA repair protein, in the nuclei of breast carcinomas is indicative of genomic instability, as we had previously documented the presence of high levels of Rad6B in the nuclei of metastatic mouse mammary tumor sublines whereas their nonmetastatic counterparts predominantly displayed cytoplasmic localization (16). Furthermore, MCF10A cells stably transfected with Rad6B with resultant high levels of nuclear Rad6B exhibited chromosomal aneuploidy, in contrast to the corresponding vector control cells that maintained the parental pseudodiploid status and cytoplasmic Rad6B (16).

Of the 12 breast carcinomas examined, ~80% of the breast tumors showed a direct association between the Rad6 and β-catenin expression, which was statistically significant ($P = 0.01$). However, an inverse correlation between Rad6 and β-catenin was found in the nontumorous ducts of a breast carcinoma wherein, besides intense membrane staining, β-catenin was also detectable in the nuclei of myoepithelial and luminal epithelial cells (Fig. 9A and A′). Whereas a breast tissue with adenosis showed moderate reactivity to both Rad6 and β-catenin antibodies (Fig. 9B and B′), five breast carcinomas (three lymph node positive and two lymph node negative) displayed intense reactivity (3+) to Rad6 and β-catenin, four showed moderate expression (2+) of β-catenin and Rad6 (two lymph node positive and two lymph node negative), one showed strong β-catenin (3+) and weak Rad6 (1+), and one showed moderate β-catenin (2+) and negligible Rad6 (0; Fig. 9G′ and G, respectively). β-Catenin was predominantly found in the cytoplasm with varying levels on the membranes; however, when present in the nucleus, β-catenin showed decreased association with the cell

membranes. Twenty-five percent of the breast carcinomas examined showed combined cytoplasmic and nuclear β-catenin and Rad6 staining in ductal carcinoma *in situ* and/or invasive cancer cells. An example of nuclear Rad6 and β-catenin is shown in Fig. 9C, C′, and D, D′. These data suggest that transcriptionally active β-catenin may play a role in activation of Rad6B promoter in at least a subset of breast tumors. Although 50% of the breast carcinomas analyzed were estrogen receptor-α positive, Rad6 and β-catenin expression did not correlate with estrogen receptor-α status of the tumors. Because the number of samples analyzed was small, the relationship between Rad6/β-catenin expression and nodal status or metastasis to other organs could not be made.

Discussion

In this study, we sought to establish the molecular basis for Rad6B overexpression in human breast cancer cells and tissues. The *Rad6B* gene does not contain a canonical TATA box, is GC-rich, and contains several putative SP1 sites. All of these features are characteristic of housekeeping genes that are constitutively active. However, dramatic increases in *Rad6B* gene expression are observed between normal and tumor breast tissues; such changes would seem to be incompatible with the notion of *Rad6B* as a housekeeping gene. Our data from functional promoter assays show that Rad6B promoter activity is negatively influenced by TCF binding. Mutation of sequences containing the TCF binding site (−341) caused a dramatic induction of basal reporter gene expression while abolishing its responsiveness to β-catenin. These data indicate that TCF-4 plays an important negative regulatory role in control of *Rad6B* gene expression and activation of Rad6B promoter requires coexpression of both β-catenin and p300. Results from EMSA and UV cross-linking experiments showed that the inability to form TCF-4/β-catenin/p300 complexes in MCF10A cells is primarily due to a paucity of transcriptionally

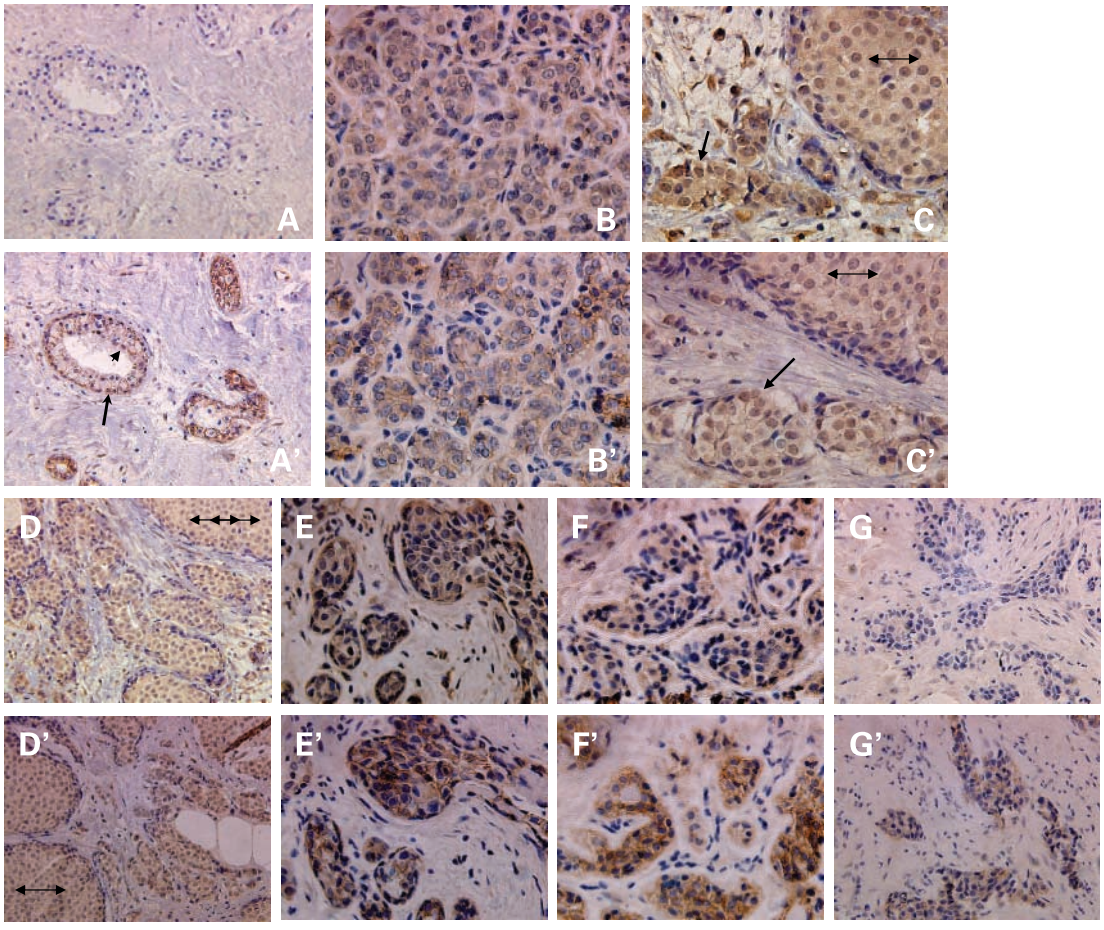

FIGURE 9. Immunohistochemical localization of Rad6 and β-catenin in human breast carcinomas. **A** to **G.** Rad6 reactivity. **A′** to **G′**. Corresponding β-catenin staining. **B** to **E** and **B′** to **E′.** Representative cases of breast tumor tissues showing a strong association between Rad6 and β-catenin. **A** and **A′.** Nontumorous ducts showing negligible Rad6 (**A**) and nuclear β-catenin expression in myoepithelial (*arrow*) and luminal epithelial (*arrowhead*) cells besides intense membrane reactivity. **B** and **B′.** Breast tissue with adenosis showing moderate cytoplasmic reactivity to Rad6 and β-catenin. **C, C′** and **D, D′.** Examples of breast carcinomas with ductal carcinoma *in situ* (*double-sided arrow*) and infiltrating carcinoma cells displaying cytoplasmic and nuclear Rad6 and β-catenin staining. **E** and **E′.** Invasive cancer cells showing cytoplasmic Rad6 and β-catenin. **F** and **F′.** Breast cancer tissue showing a weak correlation between Rad6 (1+) and β-catenin (2+) reactivity. **G** and **G′.** Breast tumor tissue showing no correlation between Rad6 and β-catenin. Magnification, ×20 (**A, A′, D, D′**, and **G, G′**); ×40 (**B, B′, C, C′, E, E′**, and **F, F′**).

active β-catenin and p300 in MCF10A nuclei and not due to deficiency of TCF-4 or inability of endogenous TCF-4 to bind to the Rad6B promoter. These data are consistent with high levels of TCF-4 expression reported in the epithelium of normal and cancerous human breast tissues (34).

Schlosshauer et al. (35) reported the presence by Western blot analysis of comparable, if not more, steady-state levels of β-catenin in MCF10A total cell lysates as compared with MDA-MB-231 cells. However, a more systematic study by Bafico et al. (36) has shown up-regulation of uncomplexed transcriptionally active form of wild-type β-catenin in ~25% of breast cancer cells lines examined including MDA-MB-231 cells. Our findings are consistent with this report in that, unlike MDA-MB-231 cells, transcriptionally active β-catenin levels are very low in MCF10A cells as shown by their diminished ability to bind to the Rad6B TCF binding sequence both *in vitro* (EMSA and UV cross-linking) and *in vivo* (chromatin immunoprecipitation), as well as to transactivate in reporter-based (Rad6B promoter and TOP/Flash) assays. TCF/LEF proteins function as transcriptional corepressors by binding to members of the Groucho/TLE family (31, 32, 37-39). Groucho/TLE proteins are general transcriptional corepressors (40-42) and have been shown to interact with histone deacteylases (39, 40), enzymes that maintain chromatin in a transcriptionally repressed state (40, 43). We have not examined whether Rad6B promoter repression observed in MCF10A cells is a result of formation of repression complexes at the TCF binding site; however, our findings suggest that activation of Rad6B promoter involves molecular switch from transcriptional repression to derepression or activation because it requires functional interaction between p300 and β-catenin. Consistent with this, chromatin immunoprecipitation experiments done with MCF10A cells cotransfected with β-catenin and p300 showed their recruitment to the Rad6B TCF binding site and induction of Rad6B promoter activity. These observations support a new concept for the pathophysiologic regulation by TCF-4/β-catenin/p300 of the *Rad6B* gene, which is involved in normal and aberrant DNA repair and ubiquitin-mediated proteolytic processes. This regulation occurs at the transcriptional level in the presence or absence of coexpressed TCF-4; however, ΔN-TCF-4 or excessive amounts of wild-type TCF-4 inhibit the β-catenin/p300–induced Rad6B promoter activity. These data suggest that besides levels of β-catenin and p300, levels of TCF-4 and potentially different isoforms of TCF that contain repressor or coactivator domains can influence the repression activity of TCF and, hence, the Rad6B promoter activity. In this regard, it is interesting to note that DNA-protein complex 1 formed from MDA-MB-231 nuclear proteins contains both TCF-4 and β-catenin whereas β-catenin immunoreactive complexes 3 and 4 lack TCF-4 immunoreactivity (Figs. 4 and 5). It is not clear at present whether this lack of TCF-4 immunoreactivity is indicative of β-catenin complex formation with another TCF isoform. Although there is considerable divergence in the 5′ untranslated region sequences of *Rad6B* genes, it is notable that the sequences corresponding to segments of human promoter (−581 to −418, −187 to −129, −88 to −50, and −28 to −1 relative to first translation start codon), as well as a putative TCF binding site, are conserved in the rat (586 bases upstream of ATG codon at base 275; accession no. U04303) and mouse (594 bases upstream of ATG codon at base 166,642; accession no. AL669920) *Rad6B* genes, further supporting their potential conserved role in regulation of *Rad6B* gene expression.

The canonical Wnt signaling pathway regulates various biological processes, including early neoplasia, by increasing the stability and transcriptional activity of the key mediator, β-catenin (44-46). Studies in mouse model systems clearly show that activation of the canonical Wnt signaling pathway leads to mammary tumorigenesis (47), and a role for β-catenin signaling in initiation of alveologenesis has been established. The mammary ducts of young virgin mouse mammary tumor virus (MMTV)-ΔN89β-catenin and MMTV-ΔN90β-catenin female mice show ductal hyperplasia, a feature consistent with early alveologenesis (48, 49). Up-regulation of β-catenin target genes, *cyclin D1* (50) and c-*myc* (51), was observed in both hyperplasia and adenocarcinoma, thus implicating β-catenin signaling in preneoplastic and neoplastic transformation (48, 49). β-Catenin-stabilizing mutations that activate Wnt signaling are frequently observed in human cancers of other tissues; however, equivalent mutations have not been detected in human breast cancers (52, 53). There is uncertainty in the literature about β-catenin deregulation in breast tumors because immunohistochemical studies of β-catenin in breast carcinomas have shown mixed results in terms of subcellular localization and correlation with other markers and patient outcome. Lin et al. (54) have reported an immunohistochemical correlation between β-catenin stabilization (cytoplasmic/nuclear localization) and cyclin D1 expression in breast cancer tissues.

Our preliminary data, although from a limited number of breast tumors, have shown that 12 of the 12 breast carcinomas examined displayed moderate to intense reactivity to β-catenin antibody, and 25% of these tumors showed combined cytoplasmic and nuclear staining. Most of the previous studies have been done on archival material whereas our present study was done on recently fixed tissues (acquired within the last 12 months), which may explain the existing uncertainty of β-catenin expression in the nucleus. It is not clear whether the breast tumor surgical specimens used by Lin et al. (54) were recently fixed tissues because the details were not provided in the article. Although the number of breast tumor tissues analyzed was small, our current study found an immunohistochemical correlation between Rad6 and β-catenin in breast carcinomas, with moderate to intense expression of both proteins in the cytoplasm and nucleus of ductal carcinoma *in situ* and invasive cancer cells. These data indicate that transcriptionally active β-catenin may contribute to the derepression/activation of Rad6B promoter in breast carcinomas, similar to our findings from reporter and DNA binding assays in MDA-MB-231 breast cancer cells. It is interesting to note that nontumorous ducts of a breast carcinoma contained nuclear β-catenin in the luminal and myoepithelial cells besides strong membrane reactivity. This early presence of nuclear β-catenin may distinguish an involved duct from a normal duct and implicate its potential transcriptional activity in up-regulation of target genes such as *Rad6B*. It is worthwhile to mention that we have thus far not encountered high Rad6

and negative β-catenin (with exclusive localization on the membranes) expression, although we have encountered moderate β-catenin and weak or no Rad6 expression. We propose that in Wnt-activated breast cancer cells, β-catenin/TCF-4 levels increase and activate TCF target genes, including *Rad6B*, which in turn contribute to lesion development in breast. A review of microarray databases failed to identify *Rad6B* among the Wnt-activated genes.[3] A plausible explanation for this may be the short half-life of *Rad6B* transcripts, which impedes the build-up of adequate steady-state levels of Rad6B mRNA, which is necessary for identification of differentially regulated genes.

Our results from *in vivo* assays showed that MCF10A cells stably overexpressing Rad6B mainly produce benign hyperplastic (grade 2) lesions, whereas lesions produced by MCF10A cells engineered to express mutant *Ha-ras* gene (33) progress to atypical ductal hyperplasia (grade 3), ductal carcinoma *in situ* (grade 4), and invasive carcinoma (grade 5). The strikingly different effects exerted by Rad6B overexpression versus oncogenic *Ha-ras* on histologic conversion and neoplastic progression of MCF10A cells are consistent with our notion that induction or deregulation of *Rad6B* gene expression is an early step in human breast carcinogenesis. These data are consistent with our previous study that showed that detectable increases in Rad6B expression occur early in benign hyperplasias with continued overexpression in ductal carcinoma *in situ* and invasive breast carcinomas (16).

Rad6 is critical for postreplication repair of DNA and maintenance of genomic integrity. However, maintenance of critical levels of Rad6 is essential as imbalances in levels of Rad6B, such as by forced overexpression in normal breast cells, induce centrosome amplification, formation of multipolar mitotic spindles, multinucleation, and aneuploidy (16). Conversely, depletion of Rad6B in normal breast cells triggers defective growth and hypersensitivity to drugs (15). Although Rad6B is a fundamental component of the postreplication repair pathway and its expression is induced by DNA-damaging drugs, our present finding that it is a transcriptional target of TCF/β-catenin shows that its expression is also regulated by oncogenic/mitogenic pathways, thus providing an alternate but important route to Rad6B transcriptional deregulation. β-catenin/TCF target genes exhibit differences in their requirement for coactivators. Our findings from the present study show that TCF/β-catenin–induced Rad6B expression is regulated in a p300-dependent fashion. A recent study showed that survivin transcription via β-catenin/TCF signaling is dependent on the coactivator cAMP-responsive element binding protein (CREB)–binding protein (CBP), and that switching from CBP to p300 at the survivin promoter is associated with its transcriptional repression (55). Whether similar cooperation of β-catenin with CBP or other transcription factors modulates Rad6B expression will require further study.

A larger study covering a wider spectrum of breast tumor types and grades is under way to further authenticate the β-catenin and Rad6B expression profiles. In summary, this is the first report that provides evidence for a potential β-catenin-mediated mechanism for Rad6B overexpression that may be operative in a subset of breast tumors.

Materials and Methods

Reagents

Antibodies were purchased as follows: anti-β-catenin mouse monoclonal antibody (clone 15B8; epitope not described; Sigma, St. Louis, MO); anti-TCF-4 (13027X; rabbit polyclonal antibody recognizes epitope corresponding to amino acids 486-610 mapping near the COOH terminus of human TCF-4; Santa Cruz Biotechnology, Santa Cruz, CA); anti-p300 (Santa Cruz Biotechnology); anti-β-actin (Sigma); and control rabbit and mouse antibody (Zymed, San Francisco, CA). pCMV-β-catenin encoding full-length human β-catenin, pCDNA3/myc-human TCF4, and pCDNA3-myc-ΔN human TCF-4 (lacking the NH_2-terminal 30 amino acids) were generously provided by Dr. Bert Vogelstein (Johns Hopkins University, Baltimore, MD). pRV-RSV-HA-p300 was supplied by Dr. Richard Goodman (Vollum Institute, Oregon Health Sciences University, Portland, OR). Reporter plasmids pFOP/FLASH and pTOP/FLASH containing the consensus mutant and wild-type TCF binding elements, respectively, were purchased from Upstate Biotechnology (Lake Placid, NY).

Cells and Cultures

MCF10A cells were cultured in DMEM/F-12 supplemented with 5% horse serum, 10 μg/mL insulin, 0.02 μg/mL epidermal growth factor, 0.5 μg/mL hydrocortisone, 0.1 μg/mL cholera toxin, 100 units/mL penicillin, and 100 μg/mL streptomycin (16). MDA-MB-231 and SW480 cells were cultured in DMEM supplemented with 5% fetal bovine serum.

Construction of Rad6B Promoter Reporter

Cells were transfected with full-length (722 bp) and truncated (560, 410, 335, and 218 bp) human Rad6B promoter fragments that were subcloned upstream of a promoterless luciferase reporter construct pGL3-Luc (Promega, Madison, WI). Plasmids are named according to the length of the 5′ untranslated region relative to the translation start codon (Fig. 1A). The forward primers used were 5′-gctgttgattctgccatgacctc-3′ (−712/−690), 5′-acgcgtcatagggacacgtggttc-3′ (−550/−527), 5′-ccccgccgagcctaaactagtg-3′ (−401/−380), 5′-tctagtctgaacacagaga-3′ (−325/−307), and 5′-cagcactcacactgtggtagcg-3′ (−208/−187). The antisense primer was 5′-ggtcgacatgctccgcagctg-3′ (+9/−12). The template was genomic DNA from MCF10A cells. The promoter fragments were subcloned into pCRII TA cloning vector (Invitrogen, Carlsbad, CA), digested with *Xho*I/*Hin*dIII, and cloned into the *Xho*I/*Hin*dIII sites of the pGL3-Basic reporter vector (Promega). All constructs were confirmed by sequencing in both directions.

Site-Directed Mutagenesis

The mutant (−712/+9) full-length Rad6B promoter was generated by site-directed mutagenesis of wild-type template DNA (pGL3−722/+9) with a single mutagenic oligonucleotide for PCR amplification followed by digestion with *Dpn*I of template DNA. The conditions used for PCR in a total volume of 50 μL were as follows: 100 ng of template DNA, 20 pmol mutagenic primer, 5 μL of 10× Pfu buffer, 25 mmol/L of each deoxynucleotide triphosphate, and 2.5 units of Pfu polymerase. The conditions for PCR amplification were 95°C, 2 minutes

followed by 18 cycles consisting of 1 minute at 95°C, annealing at 48°C for 2 minutes, and extension at 68°C for 10 minutes where the extension step is twice the length of the plasmid in kilobase in minutes. Final extension was done at 68°C for 20 minutes. Sequence integrity and the presence of the correct mutation at the TCF site (CTTTGAA→ggggGAA) were verified by sequence analysis. Mutant Rad6B promoter (−401/+9) was generated by PCR amplification from pGL3-TCF mutant −712/+9 as template, subcloned into pCRII vector, and subsequently cloned into the *Xho*I/*Hin*dIII sites of pGL3-Basic vector as described above.

Transient Transfections

Transient transfections were done using Metafectene (Biontex, Munich, Germany). Cultured cells at 70% confluence in 35-mm culture dishes were cotransfected with 2 μg of Rad6B promoter reporter constructs or the empty vector and 0.2 μg of the pRL-TK vector, a Renilla luciferase control reporter vector (Promega) used to normalize for transfection efficiency. To evaluate the transcriptional activity of endogenous TCF/β-catenin, MCF10A or SW480 cells were transfected with 1.0 μg of TOP/FLASH or FOP/FLASH. The ability of endogenous TCF to be transactivated by ectopic β-catenin was tested in MCF10A cells transfected with TOP/FLASH in the presence of β-catenin (0.25 μg), and the specificity of β-catenin stimulated response was tested by cotransfection of equivalent amounts of wild-type or ΔN-TCF plasmids. To determine whether the putative TCF site on the Rad6B promoter is functional, MCF10A or MDA-MB-231 cells were cotransfected with wild-type or mutant TCF Rad6B promoter in the presence of β-catenin (0.25 and 0.5 μg), p300 (0.25 and 0.5 μg), a combination of β-catenin and p300, or a combination of β-catenin, p300, and 2 μg of ΔN-TCF-4 or wild-type TCF-4. For all cotransfection experiments, the total mass of DNA was kept constant by including appropriate amounts of the respective control vectors. At 45 hours after transfection, the cells were lysed and the luciferase activity was measured using the Promega Dual Luciferase Assay system. Absolute promoter firefly luciferase activity was normalized against Renilla luciferase activity to correct for transfection efficiency. Triplicate dishes were assayed for each transfection and at least four to six independent transfection assays were done for each reporter construct. Effects of ectopic β-catenin, p300, and TCF-4 on *Rad6B* gene expression were determined by RT-PCR and Western blot analysis.

EMSA

A double-stranded oligonucleotide (5′-gtgtttctgtttcgt-ggtctttgaatccacaacctctag-3′) containing the putative TCF/LEF binding site (underlined) was used as the probe. The double-stranded oligonucleotide was end labeled with [γ?-^{32}P]ATP and T4 polynucleotide kinase. Binding reactions were done for 15 minutes at 30°C by incubating 10 μg of MCF10A or MDA-MB-231 nuclear extracts and 0.1 pmol of labeled oligonucleotide in 20 μL of binding buffer [10 mmol/L Tris-HCl (pH 7.5), 50 mmol/L NaCl, 0.5 mmol/L EDTA, 0.5 mmol/L DTT, 2 μg of poly(deoxyinosinic-deoxycytidylic acid)]. Competition analysis was done by adding excess (1-5 pmol) unlabeled probe or with double-stranded oligonlucleotide (5′-gtgtttctgtttcgtggtggggaatccacaacctctag-3′) containing mutation (underlined) in the TCF/LEF binding site. Protein-DNA complexes were separated on 7% polyacrylamide gel. For supershift assays, nuclear extracts were preincubated with 0.5 μg of anti-TCF-4 or anti-β-catenin antibody, or equivalent amounts of rabbit or mouse preimmune IgG, before the addition of the labeled double-stranded oligonucleotide. The gels were dried and autoradiographed with intensifying screens at −80°C.

To directly analyze and identify protein components binding to the DNA element of gel shift assay, the protein-DNA complexes in EMSAs were separated by PAGE on mini 5% polyacrylamide gels at 150 V in 0.5× Tris-borate EDTA (45 mmol/L Tris/45 mmol/L borate/0.5 mmol/L EDTA, pH 8) at 4°C. Western blots of gel shifts were done on nitrocellulose (Schleicher & Schuell, Keene, NH) membrane at 200 mA for 2.5 hours in 15 mmol/L Tris/120 mmol/L glycine (pH 8.3) at 4°C. Under these conditions, only the proteins are bound to the membranes whereas the double-stranded oligonucleotides are not retained on the filter (confirmed by autoradiography overnight), suggesting that protein-DNA complexes dissociate during the transfer. Proteins bound to membranes were identified by immunoblotting with antibodies to β-catenin or TCF-4 and enhanced chemiluminescence reaction. Complexes formed between the detected proteins and the Rad6B DNA probe were verified by autoradiography of portions of gel from the same experiment.

UV Cross-Linking

Binding reactions were done as described above for EMSAs except that 100 μg of nuclear protein and 5 ng of radiolabeled probe were used. Following binding reactions in the presence or absence of competitor, the reaction mixtures were exposed to UV radiation (total energy, 0.25 J) in a UV Stratalinker (Stratagene, La Jolla, CA) at room temperature. UV-irradiated reactions and binding reactions not subjected to UV cross-linking were boiled in SDS-sample buffer and subjected to SDS-PAGE. Gels were dried and subjected to autoradiography or to Western blot analysis with anti-β-catenin or anti-TCF-4 antibodies.

Chromatin Immunoprecipitation

Proteins and chromatin were cross-linked by treating MCF10A (control and transfected with β-catenin/p300) and MDA-MB-231 cells with 0.5% formaldehyde for 15 minutes at room temperature before sonication in lysis buffer [10 mmol/L EDTA, 50 mmol/L Tris-HCl (pH 8.0), 1% SDS, protease inhibitor cocktail (Roche Biochemicals, Indianapolis, IN)] to achieve cross-linked DNA of ~200 to 600 bp in length (56). After centrifugation, the supernatant was diluted 10-fold with dilution buffer [1% Triton X-100, 1.2 mmol/L EDTA, 167 mmol/L NaCl, 16.7 mmol/L Tris-HCl (pH 8.0)]. Nonspecific binding was eliminated via preincubation with nonimmune IgG and protein A/G agarose at 4°C for 2 hours. Agarose beads were removed by centrifugation and 15% of the supernatant was used as input. The supernatant was incubated with indicated antibodies and protein A/G agarose overnight at 4°C. Beads were collected and sequentially washed twice with

1 mL of wash buffers [0.1% SDS, 1% Triton X-100, 2 mmol/L EDTA, 20 mmol/L Tris-HCl (pH 8.0), 150 mmol/L NaCl; same buffer with 500 mmol/L NaCl; and 0.25 mol/L LiCl, 1 mmol/L EDTA, 0.5% NP40, 0.5% sodium deoxycholate, 10 mmol/L Tris-HCl (pH 8.0)]. The immunoprecipitates were reverse cross-linked for PCR or boiled for 5 minutes in SDS-sample buffer for Western blot analysis. The bound and the input DNA were analyzed by PCR with primers (−550 to −147 relative to +1 ATG start codon) that amplify a 404-bp fragment of the human Rad6B promoter. To verify the specificity of the chromatin immunoprecipitation assay, control primers circumventing the TCF binding sequence (−1,490 to −1,180 relative to +1 ATG start codon) in Rad6B promoter were also used for PCR amplification. *In vivo* occupancy of the cyclin D1 promoter by β-catenin was verified by PCR with primers (bases 880-1,410; accession no. AF511593) encompassing the TCF (base 1,351) binding site of the human cyclin D1 promoter. PCR conditions were 95°C for 1 minute, 58°C for 2 minutes, and 72°C for 3 minutes for 35 cycles, followed by extension at 72°C for 10 minutes.

RT-PCR Analysis

DNase I–treated total RNA (2 μg) from MCF10A cells transfected with wild-type TCF-4, ΔN-TCF-4, β-catenin/p300, β-catenin/p300/wt TCF-4, β-catenin/p300/ΔN-TCF-4, or control vectors was reverse transcribed using random hexamers and Superscript II (Life Technologies, Inc., Rockville, MD). Relative levels of Rad6B mRNA expression were determined by semiquantitative RT-PCR with +391/+407 (Rad6B specific) and +541/+557 (accession no. NM_003337) as forward and reverse primers, respectively, under predetermined conditions that yield a detectable PCR product within a linear range. For determination of optimal conditions, the reverse-transcribed cDNA was diluted serially in water from 100 to 3 ng/μL and mixed in a final volume of 10 μL with 1 μmol/L primer pairs, 1 unit of Taq DNA polymerase, and 1 μCi of [α-^{32}P]dCTP. Amplification was done for 35 cycles (30 seconds at 95°C, 1 minute at 57°C, 2 minutes at 72°C) with a final extension for 10 minutes at 72°C. RT-PCR analysis of glyceraldehyde-3-phosphate dehydrogenase (*GAPDH*) cDNA was carried out for each reaction as an internal control for the amount of cDNA tested. The *GAPDH*-specific primers were forward, 5′-CATTGACCTCAACTACATGGT-3′, and reverse, 5′-GGATCTCGCTCCTGGAAGA-3′ (accession no. NM_002046). The PCR products were separated by agarose gel electrophoresis, subjected to autoradiography, and the relative intensities of the Rad6B and *GAPDH* cDNAs quantitated with NIH Imaging software.

Western Blot Analysis

Cell lysates were prepared as previously described (16) in 10 mmol/L Tris-HCl (pH 7.5)/150 mmol/L NaCl/1% Triton X-100/1 mmol/L phenyl methylsulfonyl fluoride, 1 μg/mL each of leupeptin, pepstatin, and antipain, and 1 mmol/L sodium orthovanadate from MCF10A cells transiently transfected with expression vectors for β-catenin, p300, a combination of β-catenin and p300, or corresponding control vectors. Proteins (50 μg) from each lysate were separated by SDS-PAGE and transblotted onto Immobilon-P membranes. The blots were stained with anti-Rad6 antibody. Levels of β-catenin, p300, and TCF-4 were determined with antibodies to β-catenin, p300, and TCF-4, respectively. Loading of protein was monitored by reprobing stripped membranes with anti-β-actin antibody. The Rad6 antibody was generated by multiple immunization of New Zealand white rabbits with a synthetic peptide (K plus amino acid residues 131-152; accession no. NP_003328) that is conserved 100% in mouse and human HR6B and 91% in human HR6A (16). Because the human Rad6A and Rad6B proteins share ~96% identical amino acid residues, and the synthetic peptide used for generation of Rad6B differs from Rad6A by only two amino acids, levels of Rad6 proteins expressed by Rad6A and Rad6B are not distinguishable. Thus, the 17-kDa Rad6-immunoreactive protein(s) detected in human cells is regarded as Rad6 rather than Rad6A or Rad6B (16). The relative amounts of Rad6 (HR6A/HR6B) protein(s) to β-actin bands were quantitated with NIH Imaging software. MCF10A, MCF10A cotransfected with β-catenin and p300 expression plasmids, or MDA-MB-231 cells were subjected to chromatin immunoprecipitation with anti-TCF-4 antibody or the corresponding normal IgG and immunoblotted with anti-β-catenin or anti-p300 antibodies. Before chromatin immunoprecipitation, equal input was verified by immunoblotting with anti-tubulin antibody.

Three-Dimensional Morphogenesis Assay

To determine the effects of ectopic β-catenin expression on Rad6B expression, single-cell suspensions of MCF10A cells (1×10^5) in culture medium were transiently transfected with control vector or a mixture of β-catenin and p300 expression vectors, mixed with an equal volume of 1:2 diluted Matrigel (Collaborative Biomedical Products, Bradford, MA) and seeded onto eight-chambered slides precoated with 40 μL of Matrigel (57). Culture media were replaced every third day, and on day 5 to 6, the cultures were fixed in buffered formalin and paraffin embedded. Sections were stained with antibodies to Rad6 or β-catenin, followed by biotinylated anti-rabbit IgG or anti-mouse IgG, respectively, and horseradish peroxidase–conjugated streptavidin. Nuclei were counterstained with hematoxylin. The transiently transfected cells were also seeded on coverslips and monolayers assessed for expression/distribution of β-catenin by immunofluorescence staining. Nuclei were stained with 4′,6-diamidino-2-phenylindole.

Immunohistochemistry

Formalin-fixed, paraffin-embedded 5-μm breast carcinoma sections were incubated with anti-Rad6 or anti-β-catenin antibodies, followed by biotinylated antirabbit or antimouse IgG secondary antibody, respectively, and horseradish peroxidase–conjugated streptavidin. Staining was visualized with 3,3′-diaminobenzidine and nuclei were counterstained with hematoxylin. Slides were also stained in the absence of primary antibody to evaluate nonspecific secondary antibody reactions. The staining for estrogen receptor-α protein had been done during the initial pathologic evaluation for diagnostic purposes. Of the 12 breast cancer tissues, five

were lymph node–positive invasive carcinomas; four, lymph node–negative invasive carcinomas; two, lymph node–negative cases with ductal carcinoma *in situ* and invasive cancer; and one, benign breast tissue with adenosis. Areas of predominant staining patterns were visually scored and the staining intensity was graded on a scale of 0 to 3+ (0, negative; 1, weak; 2, moderate; 3, intense). χ^2 test was done to assess the significance of the association between Rad6 and β-catenin. The analysis was repeated in the subgroups classified by estrogen receptor-α status. $P < 0.05$ was considered statistically significant.

In vivo *Assay*

Female Ncr Nude mice were obtained commercially (Taconic, Germantown, NY). MCF10A-Rad6B-overexpressing cells (1×10^7/0.2 mL; ref. 16) were suspended in Matrigel and injected subcutaneously into the mammary fatpad ($n = 10$) or flank ($n = 5$). Control group consisted of vector-transfected MCF10A cells (MCF10A-Neo; $n = 10$). Animals were examined twice weekly for xenograft growth at the site of the injection. Ten weeks following injection, all mice were sacrificed by cervical dislocation, according to the NIH guidelines for the humane use of animals, and tissues from the injection site were excised and fixed in neutral buffered formalin. Paraffin-embedded, H&E-stained tissue sections of grafts were microscopically examined and graded as previously described (33). Sections were examined for proliferation and Rad6B expression by staining with anti-PCNA and anti-Rad6 antibody, respectively, and detected by the avidin-biotin method (Vector, Burlingame, CA).

Acknowledgments

We thank Dr. Bert Vogelstein for generously providing expression vectors for β-catenin, wild-type hTCF, and ΔN-hTCF; Dr. Richard Goodman for the p300 expression vector; and Dr. Gloria Heppner for critically reviewing the manuscript.

References

1. Lawrence CW. The Rad6 DNA repair pathway in *Saccharomyces cerevisiae*: What does it do, and how does it do it? BioEssays 1994;16:253–8.

2. Reynolds P, Weber S, Prakash L. Rad6 gene of *Saccharomyces cerevisiae* encodes a protein containing a tract of 13 consecutive aspartates. Proc Natl Acad Sci U S A 1985;82:168–72.

3. Jentsch S, McGrath JP, Varshavsky A. The yeast DNA repair gene RAD6 encodes a ubiquitin-conjugating enzyme. Nature 1987;329:131–4.

4. Haynes RH, Kunz BA. Life Cycle and Inheritance, Strathern J, Jones E, Broach J, editors. The molecular biology of the yeast *Saccharomyces cerevisiae*. Cold Spring Harbor: Cold Spring Harbor Laboratory; 1981. p. 371–414.

5. Lawrence CW. Mutagenesis in *Saccharomyces cerevisiae*. Adv Gene 1982;21:173–254.

6. Prakash S, Sung P, Prakash L. The eukaryotic nucleus. Vol I. Straus PR, Wilson SH, editors. Caldwell (NJ): Telford Press; 1990. p. 275–92.

7. Sung P, Prakash S, Prakash L. Mutation of cysteine-88 in the *Saccharomyces cerevisiae* RAD6 protein abolishes its ubiquitin-conjugating activity and its various biological functions. Proc Natl Acad Sci U S A 1990;87:2695–9.

8. Sung P, Prakash S, Prakash L. Stable ester conjugate between the *Saccharomyces cerevisiae* RAD6 protein and ubiquitin has no biological activity. J Mol Biol 1991;221:745–9.

9. Koken MHM, Reynolds P, Jaspers-Dekker I, et al. Structural and functional conservation of two human homologs of the yeast DNA repair gene RAD6. Proc Natl Acad Sci U S A 1991;88:8865–9.

10. Koken M, Reynolds R, Bootsma D, Hoeijmakers J, Prakash S, Prakash L. Dhr6, a *Drosophila* homolog of the yeast DNA-repair gene RAD6. Proc Natl Acad Sci U S A 1991;88:3832–6.

11. Reynolds P, Koken MH, Hoeijmakers JH, Prakash S, Prakash L. The rhp6+ gene of *Schizosaccharomyces pombe*: a structural and functional homolog of the RAD6 gene from the distantly related yeast *Saccharomyces cerevisiae*. EMBO J 1990;9:1423–30.

12. Koken MH, Smith EM, Jaspers-Dekker I, et al. Localization of two human homologs, HHR6A and HHR6B, of the yeast DNA repair gene RAD6 to chromosomes Xq24-25 and 5q23-31. Genomics 1992;12:447–53.

13. Roest HP, van Klaveren J, de Wit J, et al. Inactivation of the HR6B ubiquitin-conjugating DNA repair enzyme in mice causes male sterility associated with chromatin modification. Cell 1996;86:799–810.

14. Roest HP, Baarends WM, de Wit J, et al. The ubiquitin-conjugating DNA repair enzyme HR6A is a maternal factor essential for early embryonic development in mice. Mol Cell Biol 2004;24:5485–95.

15. Lyakhovich A, Shekhar MP. RAD6B overexpression confers chemoresistance: RAD6 expression during cell cycle and its redistribution to chromatin during DNA damage-induced response. Oncogene 2004;23:3097–106.

16. Shekhar MP, Lyakhovich A, Visscher DW, Heng H, Kondrat N. Rad6 overexpression induces multinucleation, centrosome amplification, abnormal mitosis, aneuploidy, and transformation. Cancer Res 2002;62:2115–24.

17. Behrens J. Control of β-catenin signaling in tumor development. Ann N Y Acad Sci 2000;910:21–33.

18. Brannon M, Gomperts M, Sumoy L, Moon RT, Kimelman D. A β-catenin/XTcf-3 complex binds to the siamois promoter to regulate dorsal axis specification in *Xenopus*. Genes Dev 1997;11:2359–70.

19. Cadigan KM, Nusse R. Wnt signaling: a common theme in animal development. Genes Dev 1997;11:3286–305.

20. Giles RH, van Es JH, Clevers H. Caught up in a Wnt storm: Wnt signaling in cancer. Biochim Biophys Acta 2003;1653:1–24.

21. Polakis P. Wnt signaling and cancer. Genes Dev 2000;14:1837–51.

22. Behrens J, von Kries JP, Kuhl M, et al. Functional interaction of β-catenin with the transcription factor LEF-1. Nature 1996;382:638–42.

23. Huber O, Korn R, McLaughlin J, Ohsugi M, Herrmann BG, Kemler R. Nuclear localization of β-catenin by interaction with transcription factor LEF-1. Mech Dev 1996;59:3–10.

24. Huelsken J, Behrens J. The Wnt signalling pathway. J Cell Sci 2002;115:3977–8. Review.

25. Peifer M, Polakis P. Wnt signaling in oncogenesis and embryogenesis—a look outside the nucleus. Science 2000;287:1606–9. Review.

26. van de Wetering M, Oosterwegel M, Dooijes D, Clevers H. Identification and cloning of TCF-1, a T lymphocyte-specific transcription factor containing a sequence-specific HMG box. EMBO J 1991;10:123–32.

27. van de Wetering M, Cavallo R, Dooijes D, et al. Armadillo coactivates transcription driven by the product of the *Drosophila* segment polarity gene dTCF. Cell 1997;88:789–99.

28. Brennan KR, Brown AM. Wnt proteins in mammary development and cancer. J Mammary Gland Biol. Neoplasia 2004;9:119–31.

29. Nusse R, Varmus HE. Wnt genes. Cell 1992;69:1073–87.

30. Tsukamoto AS, Grosschedl R, Guzman RC, Parslow T, Varmus HE. Expression of the int-1 gene in transgenic mice is associated with mammary gland hyperplasia and adenocarcinomas in male and female mice. Cell 1988;55:619–25.

31. Cavallo RA, Cox RT, Moline MM, et al. *Drosophila* Tcf and Groucho interact to repress Wingless signalling activity. Nature 1998;395:604–8.

32. Roose J, Molenaar M, Peterson J, et al. The *Xenopus* Wnt effector XTcf-3 interacts with Groucho-related transcriptional repressors. Nature 1998;395:608–12.

33. Dawson PJ, Wolman SR, Tait L, Heppner GH, Miller FR. MCF10AT: a model for the evolution of cancer from proliferative breast disease. Am J Pathol 1996;148:313–9.

34. Barker N, Huls G, Korinek V, Clevers H. Restricted high level expression of Tcf-4 protein in intestinal and mammary gland epithelium. Amer J Pathol 1999;154:29–35.

35. Schlosshauer PW, Brown SA, Eisinger K, et al. APC truncation and increased β-catenin levels in a human breast cancer cell line. Carcinogenesis 2000;21:1453–6.

36. Bafico A, Liu G, Goldin L, et al. An autocrine mechanism for constitutive Wnt pathway activation in human cancer cells. Cancer Cell 2004;6:497–506.

37. Hurlstone A, Clevers H. T-cell factors: turn-ons and turn-offs. EMBO J 2002;21:2303–11.

38. Billin AN, Thirlwell H, Ayer DE. β-Catenin-histone deacetylase interactions regulate the transition of LEF1 from a transcriptional repressor to an activator. Mol Cell Biol 2000;20:6882–90.

39. Brantjes H, Roose J, van de Wetering M, Clevers H. All Tcf HMG box transcription factors interact with Groucho-related co-repressors. Nucleic Acids Res 2001;29:1410–9.

40. Chen G, Courey AJ. Groucho/TLE family proteins and transcriptional repression. Gene 2000;249:1–16.

41. Courey AJ, Jia S. Transcriptional repression: the long and the short of it. Genes Dev 2001;15:2786–96.

42. Fisher AL, Caudy M. Groucho proteins: transcriptional corepressors for specific subsets of DNA-binding transcription factors in vertebrates and invertebrates. Genes Dev 1998;12:1931–40.

43. Narlikar GJ, Fan H-Y, Kingston RE. Cooperation between complexes that regulate chromatin structure and transcription. Cell 2002;108:475–87.

44. Dierick H, Bejsovec A. Cellular mechanisms of wingless/Wnt signal transduction. Curr Top Dev Biol 1999;43:153–90.

45. Miller JR, Hocking AM, Brown JD, Moon RT. Mechanism and function of signal transduction by the Wnt/β-catenin and Wnt/Ca^{2+} pathways. Oncogene 1999;18:7860–72.

46. Seidensticker MJ, Behrens J. Biochemical interactions in the wnt pathway. Biochim Biophys Acta 2000;1495:168–82. Review.

47. Moser AR, Hegge L, Cardiff RD. Genetic background affects susceptibility to mammary hyperplasias and carcinomas in Apc(min)/+ mice. Cancer Res 2001; 61:3480–5.

48. Imbert A, Eelkema R, Jordan S, Feiner H, Cowin P. ΔN89 β-catenin induces precocious development, differentiation, and neoplasia in mammary gland. Cell Biol 2001;153:555–68.

49. Michaelson JS, Leder P. β-Catenin is a downstream effector of Wnt-mediated tumorigenesis in the mammary gland. Oncogene 2001;20:5093–9.

50. Shtutman M, Zhurinsky J, Simcha I, et al. The cyclin D1 gene is a target of the β-catenin/LEF-1 pathway. Proc Natl Acad Sci U S A 1999;96:5522–7.

51. He TC, Sparks AB, Rago C, et al. Identification of c-MYC as a target of the APC pathway. Science 1998;281:1509–12.

52. Candidus S, Bischoff P, Becker KF, Hofler H. No evidence for mutations in the α- and β-catenin genes in human gastric and breast carcinomas. Cancer Res 1996;56:49–52.

53. Jonsson M, Borg A, Nilbert M, Andersson T. Involvement of adenomatous polyposis coli (APC)/β-catenin signalling in human breast cancer. Eur J Cancer 2000;36:242–8.

54. Lin SY, Xia W, Wang JC, et al. β-Catenin, a novel prognostic marker for breast cancer: its roles in cyclin D1 expression and cancer progression. Proc Natl Acad Sci U S A 2000;97:4262–6.

55. Ma H, Nguyen C, Lee KS, Kahn M. Differential roles for the coactivators CBP and p300 on TCF/β-catenin-mediated survivin gene expression. Oncogene 2005;24:3619–31.

56. Well J, Farnham PJ. Characterizing transcription factor binding sites using formaldehyde cross-linking and immunoprecipitation. Methods 2002;26: 48–56.

57. Muthuswamy SK, Li D, Lelievre S, Bissell MJ, Brugge JS. ErbB2, but not ErbB1, reinitiates proliferation and induces luminal repopulation in epithelial acini. Nat Cell Biol 2001;3:785–92.